Journal of Translational Medicine

RESEARCH

Open Access

SET7 lysine methyltransferase mediates the up-regulation of NADPH oxidase expression, oxidative stress, and NLRP3 inflammasome priming in atherosclerosis

Simona-Adriana Manea[1†], Mihaela-Loredana Vlad[1†], Alexandra-Gela Lazar[1], Horia Muresian[2], Maya Simionescu[1] and Adrian Manea[1*]

Abstract

Background Dysregulation of histone methylation-based epigenetic mechanisms leads to either transient or long-lasting transcriptomic alterations in vascular and immune cells with important consequences on atherosclerotic plaque development and stability. We hypothesized that the epigenetic enzyme SET7 lysine methyltransferase contributes to the up-regulation of NADPH oxidase (Nox) and NLRP3 inflammasome expression in atherosclerosis.

Methods To test this hypothesis, we examined human non-atherosclerotic and atherosclerotic tissue samples, apolipoprotein E-deficient (ApoE-/-) mice, and human macrophages (Mac) employing real-time PCR, Western blot, immunofluorescence microscopy, and histological techniques. Male ApoE-/- mice with established atherosclerosis were randomized to receive concomitant with the high-fat diet, 5 mg/kg (*R*)-PFI-2, a selective SET7 pharmacological inhibitor, or its vehicle, every other day for 4 weeks.

Results The results revealed that SET7 mRNA and protein, and H3K4me1 levels were significantly elevated in human carotid atherosclerotic lesions, aorta of atherosclerotic mice, and in cultured pro-inflammatory Mac. In the atherosclerotic mice, pharmacological blockade of SET7 catalytic activity with the specific inhibitor, significantly reduced atherosclerotic plaque development, decreased the aortic up-regulation of mRNA and protein levels of Nox catalytic subunits, mitigated the formation of NT-/4HNE-protein adducts, attenuated NLRP3 gene and protein expression, and reduced pro-caspase-1 and pro-IL18 cleavage. In polarized pro-inflammatory human M1-Mac, SET7-oriented pharmacological intervention reduced the transcriptional up-regulation of Nox catalytic subunits, NLRP3, caspase-1, IL1β, and IL18, and the secretion IL1β and TNFα. Transient overexpression of SET7 in human endothelial cells enhanced mRNA levels of Nox1, Nox2, Nox4, Nox5, and p22phox.

†Simona-Adriana Manea and Mihaela-Loredana Vlad contributed equally to this work.

*Correspondence:
Adrian Manea
adrian.manea@icbp.ro

Full list of author information is available at the end of the article

Conclusion The novel results show that SET7 regulates important mechanisms leading to enhanced formation of reactive oxygen species and pro-inflammatory cytokines release in atherosclerosis. The data recommend SET7 as a promising target for pharmacological interventions and as supportive therapeutic strategy in atherosclerotic cardiovascular diseases.

Keywords NADPH oxidase, NLRP3, Epigenetics, Histone, Atherosclerosis

Background

Alteration of vascular redox state, broadly referred as oxidative stress, is instrumental in the process of atherosclerotic plaque onset, progression, and destabilization [1, 2]. To find out supportive therapy to control atherosclerotic disease progression and clinical outcomes, the molecular sources and pathways contributing to reactive oxygen species (ROS) overproduction, ROS targets and their implication in signal transduction pathways mediating immuno-inflammatory responses have been extensively investigated [3, 4]. Hitherto, regardless of major achievements in the field, the precise molecular mechanisms leading to enhanced formation of ROS and redox alterations in atherosclerosis-associated cardiovascular disorders (CVD) are still debatable [5].

Among multiple sources of ROS production, members of the NADPH oxidase (Nox) family are particularly important due to their distinctive function, in both physiological and pathological conditions to produce superoxide anion ($O_2.^-$) and hydrogen peroxide (H_2O_2) in a highly regulated manner [6, 7]. Seven structurally and functionally-related Nox subtypes have been identified and characterized, namely Nox1, Nox2, Nox3, Nox4, Nox5, Duox1, and Duox2. Of these, the Nox1, Nox2, Nox4, and Nox5 isoforms were identified as major ROS-generating enzymes in the pathobiology of cardiovascular disorders. Nox5 gene is not encoded in the rodent genomes, and therefore its functional implication in human physiology and pathology is challenging [8]. Since excess formation of ROS is mechanistically associated with all stages of atheroma formation, pharmacological targeting of Nox enzymatic activity took central stage in the development of CVD therapeutic approaches [9–12]. Equally important, several molecular mechanisms mediating the up-regulation of Nox expression, such as transcription factors and specific epigenetic mechanisms have been proposed as potential therapeutic targets to prevent or attenuate the adverse effects of amplified Nox-derived ROS formation in CVD [13]. However, in-depth understanding of transcriptional regulatory processes converging to enhanced expression of Nox subtypes, a condition that favours an augmented/sustained generation of ROS, could lead to the development of targeted and effective therapies to mitigate oxidant insults in CVD.

Emerging evidence indicates that CVD-associated risk factors trigger epigenetic-related transcriptional alterations and metabolic reprogramming in both vascular and immune cells with significant consequences on the atherosclerotic plaque formation and outcome [14]. Yet, the potential role of epigenetic mechanisms in the regulation of Nox expression in atherosclerosis, and cardiometabolic disorders in general, is still debatable. Within epigenetic system, histone post-translational modifications (e.g., acetylation, methylation) are important regulators of chromatin conformation and function. Depending on the pathophysiological context, acetylation or methylation of certain amino-acid residues on nucleosomal histones leads to either transient or long-lasting transcriptomic alterations reflected in enhanced gene expression or repression in vascular wall cells and immune cells. Unlike highly dynamic and relatively unspecific histone acetylation-induced transcriptional responses, methylation of histones seems to be more stable and locus-specific epigenetic marks, suggesting a profound implication of histone methylation-based regulatory mechanisms in organizing the expression and function of the target genes at genome-wide scale [15, 16]. Highly complex enzymatic systems regulate the status of histone methylation across gene promoters and enhancers, namely, histone methyltransferases ("writers") and histone demethylases ("erasers"). Specific histone methylation marks or their multivalent combinations, also known as "epi-mutations", are recognized by specific "reader" proteins that control the expression of target genes by modulating the formation of active transcriptional complexes and the catalytic activity of RNA polymerase II [17, 18].

Several histone methyltransferases have been proposed to regulate the expression of genes that could be clinically relevant in atherosclerosis-associated CVD in terms of potential therapeutic targets and cellular biomarkers [19–22]. Among these, lysine methyltransferase SET7 may play a significant role in atherogenesis. SET7-induced mono-methylation of lysine 4 on histone 3 (H3K4me1), an epigenetic tag of active gene expression, at specific sites within gene promoter and enhancer regulatory regions has been reported as relative stable epigenetic modification that possibly contribute to long-lasting transcriptional activation of target genes [23–25]. Of note, SET7 regulates the function of multiple non-histone proteins including transcription factors (e.g., NF-kB) and ribosomal proteins (e.g., eL42) leading to increased transcription of inflammation-related genes and enhanced proteins synthesis in specific pathophysiological contexts [26, 27].

Despite of the existing studies, the precise role of SET7 in mediating the up-regulation of Nox expression, oxidative stress, and inflammatory response in atherosclerosis is not entirely defined. In this context, we hypothesized that Nox genes could be important targets of SET7 leading to enhanced Nox expression, thus contributing to sustained ROS production, vascular oxidative damage, activation of inflammation-related mechanisms, and atherosclerotic lesion progression. We present here evidence that SET7 expression is up-regulated in human carotid atherosclerotic lesions, atherosclerotic aorta of hypercholesterolemic apolipoprotein E knockout (ApoE-/-) mice and in cultured pro-inflammatory macrophages (Mac). Moreover, employing a highly selective SET7 catalytic inhibitor, we discovered that SET7 contributes to up-regulation of Nox expression, oxidative stress-induced protein modifications, NLRP3 inflammasome priming and activity, and atherosclerotic lesion progression in ApoE-/- mice. We provide evidence that SET7 blockade suppresses the augmented transcription of Nox catalytic subunits and NLRP3 inflammasome in pro-inflammatory Mac. From a translational perspective, pharmacological targeting of SET7 enzymatic activity could become an important supportive therapeutic strategy to mitigate the adverse effects of oxidative stress and inflammation in atherosclerosis-related CVD.

Methods

Harvesting of human non-atherosclerotic and atherosclerotic tissue specimens

Non-atherosclerotic and atherosclerotic tissue specimens were obtained as waste biological materials from patients with severe carotid stenosis undergoing carotid endarterectomy (at University Hospital, Bucharest). A small tissue fragment derived from superior thyroid artery/STA (≈1–2 mm in length) adjacent to endendarterectomized vascular territory, not affected by the atherosclerotic process, was collected and taken as control. This sampling does not involve another incision or enlargement of the planned surgical incision. The clinical characteristics of the patients enrolled in the study are shown in Table S1. The study was done in agreement with the ethical directives for medical research implicating human subjects (The Code of Ethics of the World Medical Association, Declaration of Helsinki). Written informed consent was provided by the study patients. The experimental protocols were approved by the ethical committee of the Institute of Cellular Biology and Pathology (ICBP) "Nicolae Simionescu" (#11/29.06.2016, #03/07.04.2021).

Mouse model of atherosclerosis and treatment strategy

Male ApoE-/- mice (B6.129P2-Apoetm1Unc/J; strain number 002052) derived from Jackson Laboratory were housed and reproduced in our specific pathogen-free (SPF) animal facility. Standard rodent chow and water was administrated ad-libitum. At 8 weeks of age, the mice were fed with a normal diet (ND) or a high-fat, cholesterol rich diet (HD) for 10 weeks, to accelerate the development of aortic atherosclerotic lesions as previously described [28]. Subsequently, ApoE-/- (HD) mice with established atherosclerosis were randomized to receive concomitant with HD intervention, 5 mg/kg (*R*)-PFI-2 SET7 pharmacological inhibitor or its vehicle/Veh (5% DMSO + 95% PBS, pH 7.4) via intraperitoneal injection, every other day to reduce discomfort produced by local inflammation, for 4 weeks. ApoE-/- mice fed a ND, exhibiting reduced lipid deposits throughout the aorta, were taken as controls for atherosclerotic ApoE-/- (HD) mice. The experimental mice groups were: (i) ApoE-/- (ND) + Veh, (ii) ApoE-/- (HD) + Veh, and (iii) ApoE-/- (HD) + (*R*)-PFI-2. The optimal dose and the procedure of (*R*)-PFI-2 pharmacological compound administration to mice were established in agreement with the previously published work [29]. Animal study protocols conformed to the guidelines of EU Directive 2010/63/EU, and were approved by the ethical committee of the ICBP "Nicolae Simionescu" (#04/07.04.2021).

Cell culture experimental design

Human THP-1 monocytic cell line obtained from the American Tissue Culture Collection (ATCC®, USA) was used. To promote monocyte (Mon) differentiation to resting Mac (M0), THP-1 cells were seeded at a density of 5×10^5 cells per well into 12-well cell culture plates (3.5 cm^2 surface area/well), and exposed for 72 h to 100 nM phorbol-12-myristate-13-acetate (PMA) in RPMI-1640 medium containing 10% heat-inactivated fetal bovine serum (FBS) and 2% penicillin-streptomycin-neomycin solution [30]. Mac were subjected to a standard polarization procedure involving 72 h-exposure of cells to 100 ng/mL LPS + 20 ng/mL IFNγ to induce the pro-inflammatory (M1)-like Mac phenotype or 20 ng/mL IL-4 + 20 ng/mL IL-13 to promote the anti-inflammatory (M2)-like Mac phenotype. Mac exposed to the culture medium alone were considered as resting Mac (M0).

Mouse Mon were freshly isolated from the spleen of male C57BL6J mice fed a normal diet employing a negative selection kit (EasySep™, Stemcell™ Technologies). To trigger Mon-to-Mac differentiation, primary cultures of mouse Mon were exposed for 7 days to RPMI-1640 supplemented with 10% FBS, 10% L929 cell line (Sigma)-derived conditioned medium, and antibiotics. Thereafter, the adherent cells (Mac) were further cultured for 3 days in RPMI-1640 medium containing 10% heat-inactivated FBS and antibiotics comprising 100 ng/ml LPS + 20 ng/ml IFNγ or 20 ng/ml IL-4 to generate M1-like or M2-like Mac phenotype, respectively.

To assess the role of SET7 in mediating specific transcriptional responses associated with oxidative stress and inflammation in Mac, M0-, M1- and M2-like Mac were exposed to polarization factors in the presence/absence of SET7 pharmacological inhibitors (1 μM (*R*)-PFI-2 or 5μM sinefungin) or vehicle. In some experiments, human Mac were treated with 25 μg/ml oxLDL in the absence/presence of 1 μM (*R*)-PFI-2, for 24 h.

Human EA.hy926 cell line and human embryonic kidney 293 (HEK293) cell line derived from ATCC®, commonly acknowledged for achieving high transfection efficiency, were employed as cellular reporter system in transient transfection assays.

Microscopic examination of human tissue specimens

The general morphological aspects of the human non-atherosclerotic and atherosclerotic tissue specimens were examined after hematoxylin-eosin (H&E) staining. In brief, after surgical sampling, the tissue specimens were washed in ice-cold PBS (pH 7.4), fixed in 4% buffered-paraformaldehyde solution, and processed for frozen tissue sectioning technique. STA-derived non-atherosclerotic and carotid-artery atherosclerotic cryosections (5 μm thick) were applied onto Superfrost™ Plus microscope slides (Thermo Fisher Scientific, USA) and subjected to H&E staining according to the manufacturer's protocol (Carl Roth, Germany). The specimens were examined and photographed employing a Zeiss Axio Observer microscope (Carl Zeiss, Germany).

Immunofluorescence (IF) microscopy

Serial cryosections (5 μm thick) obtained from human non-atherosclerotic STA and carotid-artery atherosclerotic specimens, and aortic root cryosections derived from male ApoE-/- mice fed and normal or a high-fat, cholesterol-rich diet were mounted onto microscope slides and subjected to fluorescence immunolabeling for SET7 (rabbit polyclonal, PA5-97320, dilution 1:100) or H3K4me1 (rabbit polyclonal, C15410037, dilution 1:500). Alexa Fluor ™ 594 goat anti-rabbit IgG (A11037, dilution 1:500) was employed as secondary antibody. The cell nuclei were counterstained with 4′,6-diamidino-2-phenylindole (DAPI). Tissue sections were analyzed using a Leica DMi8 inverted fluorescence microscope.

Assessment of plasma cholesterol and triglyceride levels in mice

Blood samples were collected in EDTA-coated tubes (Becton Dickinson, Germany) from animals via cardiac puncture at the time of sacrifice, and plasma was obtained by centrifugation (1.000 x g, 10 min, 4°C). Total plasma cholesterol and triglyceride levels were assessed employing standard colorimetric kits in accordance with the manufacturer's technical specifications (Dialab, Austria).

Enzyme-linked immunosorbent assay (ELISA)

Quantikine® colorimetric ELISA kits were employed in agreement with the manufacturer's protocols (R&D Systems) to determine the levels of monocyte chemoattractant protein-1 (MCP-1), tumor necrosis factor α (TNFα), and interleukin 1β (IL-1β) in the plasma of mice, and IL-1β and TNFα in the culture medium derived from human Mac.

Assessment of atherosclerotic lesion formation in mice

The development of atherosclerotic lesions was examined in the aortic root by H&E staining of serial cryosections and along the aorta of mice by "*en face*" method employing Oil Red O (ORO) labelling of lipid deposits. Atherosclerotic lesional area was quantified in the aortic root and along the aorta of mice employing the ImageJ software (NIH Image, USA).

Real-time polymerase chain reaction assay (Real-Time PCR)

Total RNA was isolated from human/mouse tissue samples and cultured cells employing standard column-based RNA purification kits, namely, RNeasy® (Qiagen, Germany) for arterial tissues and GenElute™ mammalian total RNA kit for cells (Sigma, Germany). Prior to RNA extraction and purification procedure, the human and mouse arterial samples were rinsed in ice-cold PBS (pH 7.4), resuspended in QIAzol lysis solution, and subjected to tissue homogenization employing a mini-beadbeater disrupter and 1 mm diameter glass beads (BioSpec, USA). Total tissue and cellular RNA was reverse-transcribed into complementary DNA strand (cDNA) using M-MLV reverse transcriptase in accordance with the manufacturer's specifications (Thermo Fisher Scientific, USA). The cDNA was subjected to real-time PCR amplification and analysis in a LightCycler 480 II thermocycler (Roche, Switzerland), using SYBR™ Green I probe. The comparative C_T method [31] was applied to quantify the relative mRNA expression employing the β-actin transcript level as internal reference. If not specifically presented in Table S2, the sequences of the oligonucleotide primers employed in real-time PCR assays were derived from Origene (USA).

Western blot assay

Tissue and cell-derived total protein extracts were obtained as previously indicated [29]. Briefly, human and mouse arterial specimens were washed with ice-cold PBS (pH 7.4), collected in radioimmunoprecipitation assay (RIPA) buffer supplemented with protease inhibitors (Sigma, Germany), subjected to glass bead homogenization procedure (BioSpec, USA), and diluted (1:1)

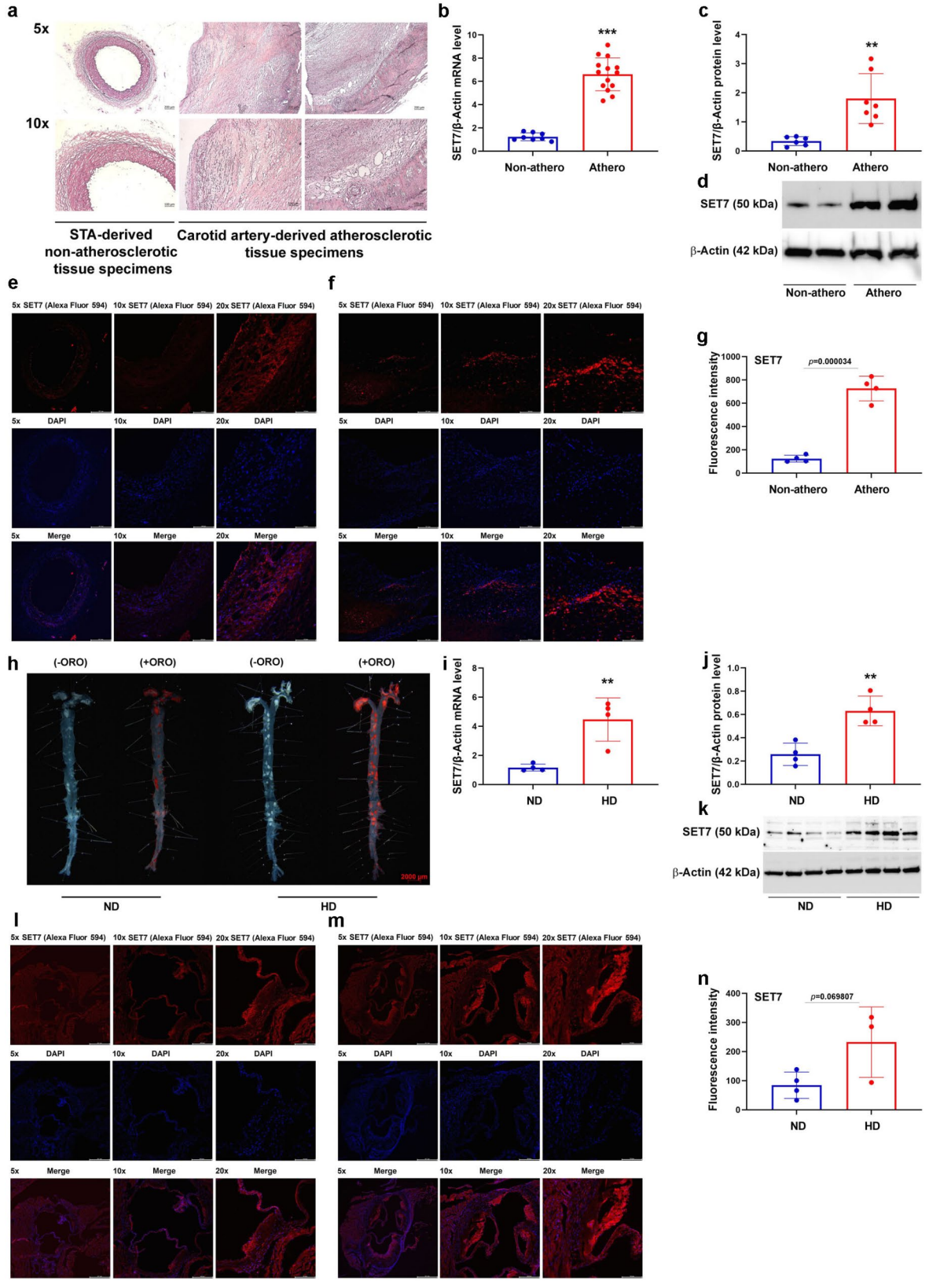

Fig. 1 (See legend on next page.)

(See figure on previous page.)

Fig. 1 SET7 expression is elevated in human carotid atherosclerotic lesions and in atherosclerotic aorta of mice. **a**, Representative microscopy images of H&E-stained non-atherosclerotic (STA) and atherosclerotic (carotid artery) tissue sections derived from a study patient photographed under 5x and 10x magnification. **b-c**, Real-time PCR and Western blot analysis depicting the up-regulation of SET7 transcript and protein levels in human atherosclerotic lesions. **d**, Representative blot showing the immunodetection of SET7 protein in non-atherosclerotic and atherosclerotic tissue homogenates. **e-f**, IF microscopy images depicting the localization of SET7 within non-atherosclerotic (left panel) and atherosclerotic tissue specimens (right panel). **g**, Quantification of SET7 probe fluorescence intensity in non-atherosclerotic and atherosclerotic specimens. **h**, En *face* examination of aortic atherosclerotic lesion development in ApoE-/- mice fed a normal (ND) or high-fat, cholesterol-rich atherogenic diet (HD) for 14 weeks, employing ORO staining of lipid deposits. The aortas were photographed in the absence (-ORO) and presence (+ ORO) of lipid staining solution. **i-j**, Gene and protein expression analysis showing the augmented aortic expression of SET7 in atherosclerotic ApoE-/- mice. **k**, Representative blot showing the immunodetection of SET7 protein in aortic tissue homogenates derived from ApoE-/- (ND) and ApoE-/- (HD) mice. **l-m**, IF microscopy images showing the localization of SET7 within aortic root-derived atherosclerotic lesions obtained from ApoE-/- (ND) **(**left panel**)** or ApoE-/- (HD) mice (right panel). **n**, Quantification of SET7 probe fluorescence intensity in atherosclerotic lesions derived from ApoE-/- (ND) and ApoE-/- (HD) mice. $n = 4–14$ (human samples), $n = 3–4$ (mouse samples), ** $p < 0.01$, *** $p < 0.001$. *p*-values were considered in relation to non-athero (human samples) or ND (mouse samples) condition. Non-athero, non-atherosclerotic STA control tissue samples

in 2xLaemmli's buffer (Serva, USA). Cultured Mac and HEK293 cells were washed with PBS (pH 7.4), resuspended in Laemmli's buffer containing protease inhibitors. Tissue and cell culture-derived protein lysates were incubated at 95 °C for 20 min, separated by SDS-PAGE (30 µg protein/lane), and electroblotted onto nitrocellulose membranes (Bio-Rad, USA). The membranes were exposed for 12 h at 4 °C to the following primary antibodies diluted in TBS blotto A blocking buffer (sc-2333): SET7 (rabbit polyclonal, PA5-97320, dilution 1:500), Nox1 (rabbit polyclonal, ab131088, concentration 0.5 µg/mL), Nox2 (mouse monoclonal, sc-130543, dilution 1:200), Nox4 (rabbit polyclonal, sc-30141, dilution 1:200), p22phox (mouse monoclonal, sc-271262, dilution 1:200), nitrotyrosine/NT (mouse monoclonal, MAB3248, concentration 1 µg/mL), 4-hydroxynonenal/4-HNE (mouse monoclonal, MAB3249, concentration 1 µg/mL), NOS2 (mouse monoclonal, sc-7271, dilution 1:200), NLRP3 (rabbit monoclonal, ab263899, dilution 1:1000), caspase 1 (mouse monoclonal, MA5-16215, concentration 1 µg/mL), IL18 (rabbit polyclonal, PA5-76082, dilution 1:500), H3K4me1 (rabbit polyclonal, C15410037, dilution 1:500), histone H3 (mouse monoclonal, C15200011, dilution 1:1000), and β-actin (mouse monoclonal, sc-47778, dilution 1:500). Anti-rabbit IgG-HRP (sc-2370, dilution 1:5000) and anti-mouse IgG-HRP (sc-2031, dilution 1:5000) were employed as secondary antibodies. The nitrocellulose membranes were washed, exposed to SuperSignal™ solution, and the protein bands were detected employing an ImageQuant LAS 4000 digital chemiluminescence detection system (Fujifilm, Japan). Densitometric analysis was performed by using TotalLab Quant software. The β-actin or histone H3 protein levels were used for internal normalization.

Transfection assay

Transient transfection of EA.hy926 and HEK293 cells was performed using Viromer® Red reagent (Origene, USA). Twenty-four hours before transfection, the cells were seeded at density of 1×10^5 cells per well into 12 multiwell plates (3.5 cm^2 surface area/well) and transfected with 11 ng/µL pCMV6-Entry (empty vector control) or pCMV6-SET7 (NM_030648) to overexpress human SET7 lysine methyltransferase (Origene, USA). Twenty-four hours after transfection, EA.hy926/HEK293 cells underwent neomycin selection for 3 days. The resulting neomycin-resistant cells were further considered to investigate transcriptional regulation of Nox catalytic subunits or specific markers of vascular inflammation by SET7.

Statistical analysis

Data generated from at least three independent samples are presented as mean ± standard deviation (SD). The statistical differences among experimental groups were evaluated by two-tailed *t-test* and one-way analysis of variance (ANOVA) followed by Tukey's *post hoc* test. Statistical significance was considered at $p < 0.05$.

Results

SET7 expression is up-regulated in human and mouse atherosclerotic arteries

To investigate the clinical relevance of SET7 lysine methyltransferase, we performed an initial morphological examination and the gene and protein expression profiling of human carotid atherosclerotic lesions and STA-derived non-atherosclerotic tissue specimens, taken as controls. Histological examination (H&E staining) of carotid artery-associated atherosclerotic plaque demonstrated complex morphological alterations characteristically related to calcified fibro-lipid atherosclerotic plaques, enhanced immune cell infiltration and the presence of intraplaque neovessels. In contrast, in controls, microscopic analysis of H&E-stained tissue specimens revealed the absence of atherosclerotic plaques or of structural modifications of the arterial wall (Fig. 1a).

By real-time PCR and Western blot assays we determined a significantly higher SET7 mRNA (≈ 5.3-fold) and protein (≈ 5-fold) expression levels in human carotid atherosclerotic lesions when compared with controls, the STA samples (Fig. 1b-d). In addition, the level of H3K4me1, a histone modification typically catalyzed by

SET7, was found significantly elevated in atherosclerotic tissue homogenates (Figure S1).

IF microscopy examination revealed that SET7 is broadly expressed in vascular cells within non-atherosclerotic arterial wall and in the area of infiltrated immune cells in human atherosclerotic lesions (Fig. 1e and f). Noteworthy, unlike other lysine methyltransferases, SET7 does not contain protein domains to signal nuclear localization and export. Hence, SET7 protein has been previously detected in the both cytoplasm and nucleus in various cell types [24]. A similar pattern of H3K4me1 localization was detected in non-atherosclerotic or atherosclerotic specimens (Figure S2a and b). Moreover, significant increases in SET7 and H3K4me1 probe fluorescence intensity were determined in cross sections of human atherosclerotic lesions as compared to non-atherosclerotic arterial specimens (Fig. 1g and Figure S2c).

In view of further functional and mechanistic studies we next questioned whether a similar SET7 expression pattern is present in an experimental model of atherosclerosis, namely, ApoE-/- mice. To accelerate the formation of atherosclerotic lesions, ApoE-/- mice were fed a high-fat, cholesterol-rich diet (HD) for 14 weeks in accordance with the previously published standard protocol [28]. *En face* examination (Oil Red O staining) confirmed the development of atherosclerotic lesions in the aortic root and all over the aorta of ApoE-/- (HD) mice. In contrast, mice maintained on standard rodent chow diet exhibited moderate lipid deposits typically located in aortic arch and to a lesser extent along the aorta ramifications (Fig. 1h). Compared to littermate control (ApoE-/- mice fed normal diet), the atherosclerotic aortas derived from ApoE-/- (HD) mice exhibited significant increases in SET7 mRNA (≈4-fold) and protein (≈2.5-fold) levels (Fig. 1i-k), and H3K4me1 (Figure S1). SET7 (Fig. 1l and m) and H3K4me1 immunostaining (Figure S2d and e) was evident within aortic root-derived atherosclerotic lesions in ApoE-/- (ND) and ApoE-/- (HD) mice. Augmented SET7 and H3K4me1 protein levels correlated with the severity of aortic root atherosclerotic lesions in ApoE-/- mice (Fig. 1n and Figure S2f). These data demonstrate that, both clinically and experimentally, the advanced atherosclerotic lesions are associated with enhanced SET7 gene and protein expression.

Pharmacological Blockade of SET7 catalytic activity reduces atherosclerotic lesion development in ApoE-/- mice

To determine whether a functional correlation between the up-regulated SET7 expression and atherosclerotic plaque development exists, pharmacological inhibition studies on atherosclerotic ApoE-/- mice were performed [28, 32] using a highly specific SET7 catalytic inhibitor, namely, (*R*)-PFI-2. A schematic representation of the experimental approach and animal treatment strategy is shown in Fig. 2a. Atherosclerotic lesions were examined in both aortic root (H&E staining) and throughout the aorta (*en face*, Oil Red O staining) of mice. We found that as compared with ApoE-/- (ND) control mice, significant increases in atherosclerotic lesion development were present in the aortic root (≈2-fold) and along the entire aortas (≈4-fold) derived from ApoE-/- (HD) mice. Of note, atherosclerotic lesion progression was significantly reduced in response to SET7 inhibitor ((*R*)-PFI-2) treatment in both aortic root and aorta of ApoE-/- (HD) mice (Fig. 2b-e). Plasma total cholesterol and triglyceride levels were not significantly affected by the SET7-oriented pharmacological intervention in ApoE-/- (HD) mice. No significant changes in body weights were determined between the experimental groups (Fig. 2f-h).

To explore the potential regulatory effect of (*R*)-PFI-2 treatment on systemic inflammation, we measured the plasma levels of MCP-1, TNFα, and IL1β in each experimental condition. MCP-1, TNFα, and IL1β levels were found significantly elevated in the plasma of ApoE-/- (HD) mice as compared to ApoE-/- (ND) animals. No significant changes in MCP-1, TNFα, and IL1β plasma levels were determined in (*R*)-PFI-2-treated ApoE-/- (HD) mice as compared to vehicle-treated ApoE-/- (HD) mice (Figure S3).

These data suggested that up-regulated SET7 drives epigenetic alterations in the aorta of mice resulting in local rather than systemic transcriptional control of a number of genes that are mechanistically associated to atherosclerotic plaque development.

SET7 mediates the up-regulation of Nox expression in the atherosclerotic aorta of ApoE-/- mice

Enhanced production of ROS driven by up-regulated Nox plays an important role in the pathoetiology of atherosclerosis by complex mechanisms involving the activation of redox-sensitive pro-inflammatory signalling pathways, oxidative stress-induced structural alteration of molecules, and cell damage [33]. Therefore, we next questioned whether dysregulated SET7 contributes to the up-regulation of Nox expression in experimental atherosclerosis. By real-time PCR and Western blot assays, we found significantly augmented mRNA and protein levels of Nox1 (mRNA: ≈ 3-fold; protein: ≈ 2.5-fold), Nox2 (mRNA: ≈ 2-fold; protein: ≈ 2-fold), and Nox4 (mRNA: ≈ 4-fold; protein: ≈ 2-fold) catalytic subunits, as well as of p22phox essential subunit (mRNA: ≈ 4.5-fold; protein: ≈ 2.5-fold) in the atherosclerotic aorta of hypercholesterolemic ApoE-/- (HD) mice compared to controls, the ApoE-/- (ND) mice.

Interestingly, the inhibition of SET7 catalytic activity significantly reduced the up-regulation of Nox

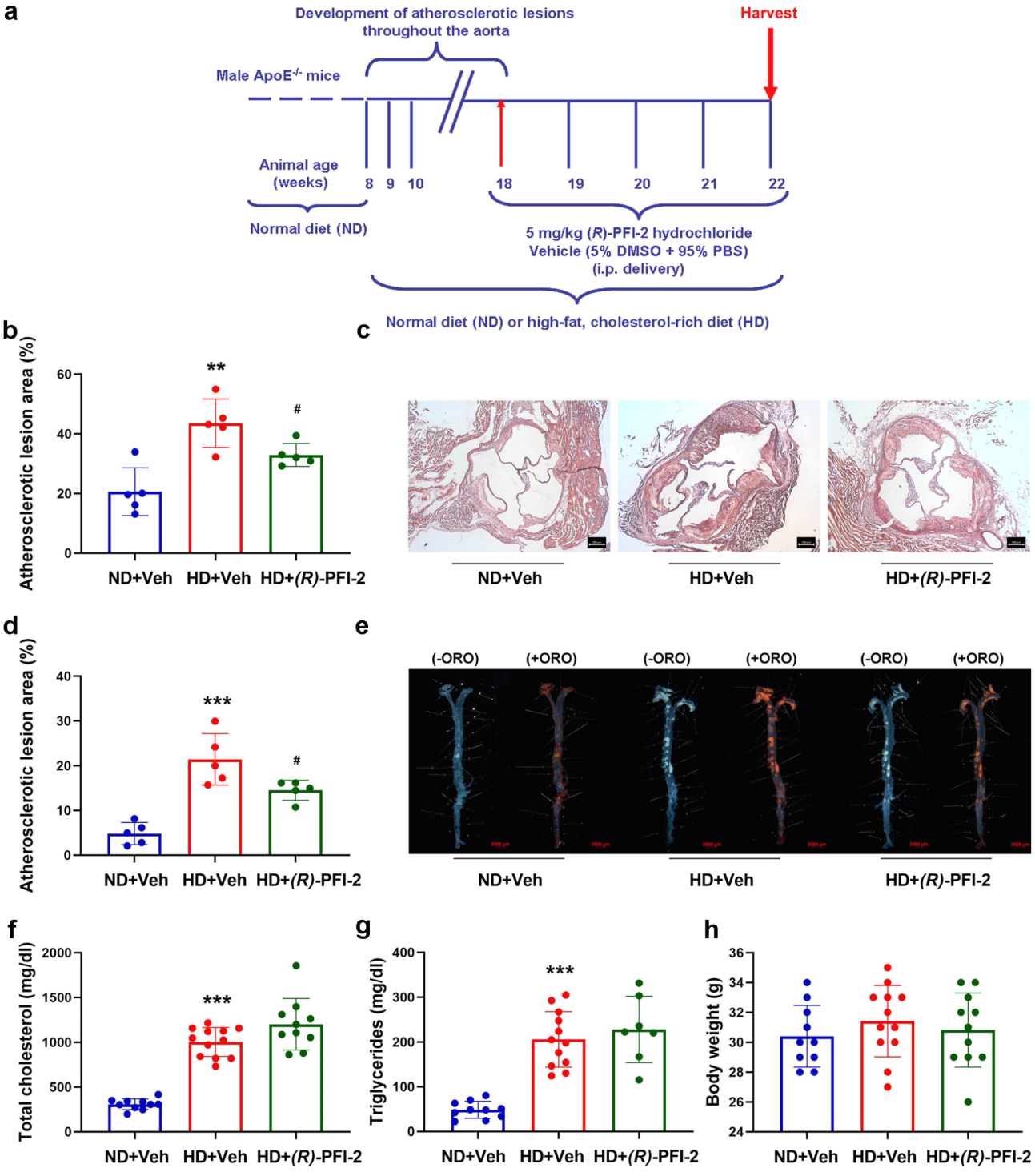

Fig. 2 Pharmacological inhibition of SET7 catalytic activity reduces the development of atherosclerotic lesions in ApoE-/- mice. **a**, Schematic overview of the general experimental strategy. **b**, Quantification of atherosclerotic lesions in aortic root. **c**, Representative images depicting H&E-stained aortic root atherosclerotic plaques. **d**, Quantification of *en face* ORO-positive areas in the aorta of ApoE-/- mice. **e**, En face examination of atherosclerotic lesion development along the aorta of mice. Images were taken in the absence (-) ore presence (+) of ORO lipid staining reagent. **f**, Assessment of plasma total cholesterol, triglycerides and body weight of mice at the moment of sacrifice. $n = 5–12$, ** $p < 0.01$, *** $p < 0.001$. *p*-values were considered in relation to ND + Veh condition. # $p < 0.05$. *p*-values were considered in relation to HD + Veh condition

subunit expression in the aorta of atherosclerotic mice (Fig. 3). These findings indicated that the activation of SET7-related mechanisms contribute to Nox up-regulation and potentially sustained ROS overproduction in atherogenesis.

Inhibition of SET7 catalytic activity mitigates the formation of NT- and 4HNE-protein adducts in the aorta of atherosclerotic mice

Nox-derived ROS contribute to peroxynitrite anion (ONOO-) and the lipid peroxidation product 4-hydroxynonanale (4HNE) formation, relevant biomarkers of oxidant milieu in atherosclerosis [33]. To evaluate the potential role of SET7 in mediating oxidative stress-induced protein structural alterations, the accumulation of NT- and 4HNE-protein adducts was determined by Western blot assay in mouse aortic tissue homogenates. Augmented levels of NT- (≈3-fold) and 4-HNE-modified protein (≈2-fold) were determined in the atherosclerotic mouse aorta, which were significantly attenuated by SET7 inhibition (Fig. 4). It is worth mentioning that, the aortic expression of inducible nitric oxide synthase (NOS2), a key source of NO implicated in ONOO- formation under pro-oxidant environment was also significantly reduced in response to SET7 pharmacological inhibition in atherosclerotic mice (Figure S4). These data point to SET7 as a novel potential therapeutic target to mitigate oxidative stress-associated structural-functional alteration of proteins in atherosclerosis.

SET7 mediates the up-regulation of NLRP3 expression in the atherosclerotic aorta of mice

Dysregulated vascular redox state and enhanced inflammatory response are considered interrelated processes in atherosclerosis [34]. Thus, we tested the potential implication of SET7 in mediating NLRP3 inflammasome priming, an important mechanism leading to enhanced pro-inflammatory cytokine secretion, namely, IL1β and IL18 [35–37]. Compared to control mice [[ApoE-/- (ND)], significantly higher transcript levels of NLRP3 (≈2.5-fold), Casp1 (≈3-fold), IL1β (≈2.5-fold) and IL18 (≈1.5-fold) were detected in atherosclerotic aorta of mice exposed to high fat diet [ApoE-/- (HD)]. Interestingly, pharmacological inhibition of SET7 by (*R*)-PFI-2 intervention prevented the induction of NLRP3 and Casp1 transcription in the aorta of atherosclerotic mice, and had no significant effects on IL1β and IL18 mRNA levels (Fig. 5a-d). To further explore the potential involvement of SET7 signalling in the regulation of NLRP3 inflammasome activation we analyzed by Western blot the protein expression profile of NLRP3, Casp1 and IL18 in aortic homogenates. Elevated protein levels corresponding to NLRP3 (≈2-fold), and active forms of Casp1 (≈3-fold) and IL18 (≈2.5-fold) were found in the atherosclerotic aorta of ApoE-/- (HD) mice. The (*R*)-PFI-2 intervention significantly reduced pro-Casp1 and pro-IL18 cleavage to active Casp1 and IL18, respectively, in the aorta of atherosclerotic mice. The levels of pro-Casp1 and pro-IL18 proteins were not significantly affected by SET7 blockade

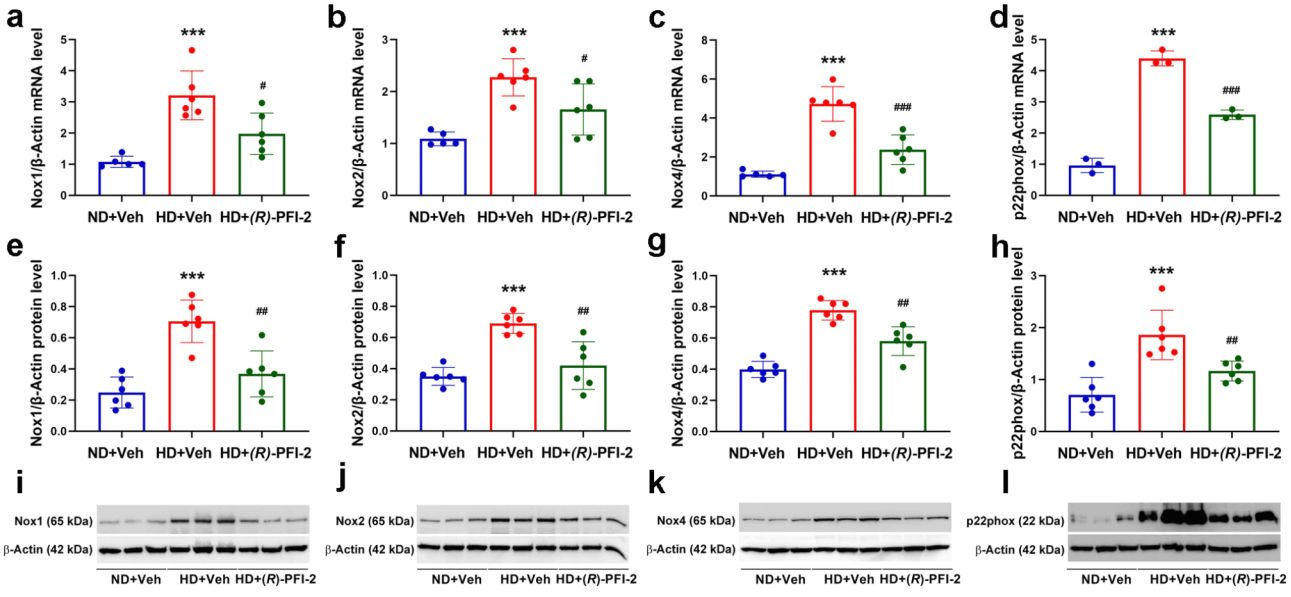

Fig. 3 SET7 mediates the up-regulation of Nox catalytic subunit expression in the atherosclerotic aorta of mice. **a-d**, Gene expression analysis depicting the down-regulatory effects of (*R*)-PFI-2 pharmacological intervention on Nox1, Nox2, Nox4, and p22phox transcript levels. **e-h**, Western blot-related densitometric analysis showing the attenuation of aortic Nox1, Nox2, Nox4, and p22phox protein levels in atherosclerotic mice in response to SET7 pharmacological blockade. **i-l**, Representative blots illustrating the immunodetection of Nox1, Nox2, Nox4, and p22phox proteins in aortic tissue homogenates. $n = 3–6$, *** $p < 0.001$. *p*-values were considered in relation to ND + Veh condition. # $p < 0.05$, ## $p < 0.01$, ### $p < 0.001$. *p*-values were considered in relation to HD + Veh condition

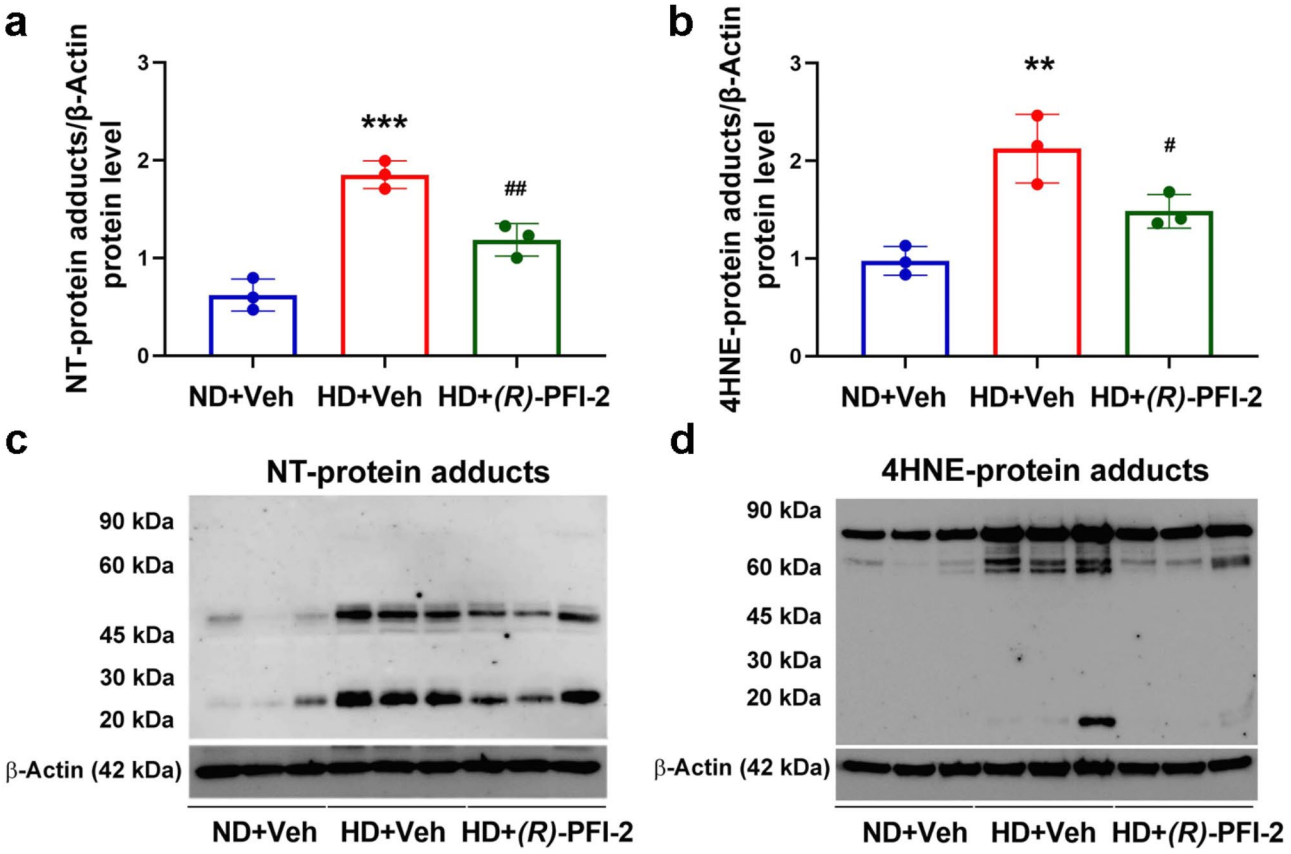

Fig. 4 Blockade of SET7 function reduces NT-/4HNE-protein adducts formation in the atherosclerotic aorta of mice. **a-b**, Western blot quantification of NT-/4HNE-modified protein levels. **c-d**, Representative immunoblots depicting protein bands reflecting the status of protein tyrosine nitration and the formation of 4HNE-histidine adducts in the aortas. $n = 3$, ** $p < 0.01$, *** $p < 0.001$. *p*-values were considered in relation to ND + Veh condition. # $p < 0.05$, ## $p < 0.01$. *p*-values were considered in relation to HD + Veh condition

in the aorta of ApoE-/-(HD) mice (Fig. 5e-i). These data indicate that SET7 contributes to the inflammatory response in atherosclerosis by mediating NLRP3 inflammasome priming and activation.

SET7 expression is up-regulated in pro-inflammatory macrophages

SET7 is a ubiquitously expressed epigenetic enzyme that has pleiotropic functions in the regulation of gene expression and protein synthesis. Thus, several cell types are likely to contribute to the overall regulatory effects of SET7 detected in the whole arterial tissue. Among other cell types, Mac are important sources of ROS, cytokines and chemokines with major functional implications in plaque development. It is worth mentioning that both Nox and NLRP3 inflammasome are expressed at high level in Mac. Thus, to complement the in vivo studies we focused on cultured Mac (as a basic in vitro experimental set-up) to investigate SET7-mediated transcriptional effects. Since two major Mac populations with divergent functional characteristics exist in the atherosclerotic lesions, an in vitro model of Mac polarization was employed to obtain M0, M1 and M2-Mac. Gene expression profiling demonstrated a typical transcriptional pattern defining a pro-inflammatory M1 phenotype, namely augmented MCP-1, TNFα and NOS2 mRNA levels. The anti-inflammatory M2 phenotype was characterized by up-regulated CD163, CD206, and MERTK mRNA levels. Noteworthy, significantly higher SET7 mRNA (≈ 2.5-fold) and protein (≈ 1.25-fold) expression levels were determined in M1-Mac when compared with resting M0-Mac. A significant ≈ 2.5-fold induction of H3K4me1 level, a histone modification directly associated with SET7 catalytic function, was measured in M1-Mac as related to H3K4me1 status detected in M0-Mac. Interestingly, pharmacological inhibition of SET7 resulted in a significant decrease in IL1β and TNFα secretion in the culture medium derived from M1-Mac (Fig. 6). The data revealed that up-regulated SET7 expression and activity was associated with a pro-inflammatory Mac phenotype.

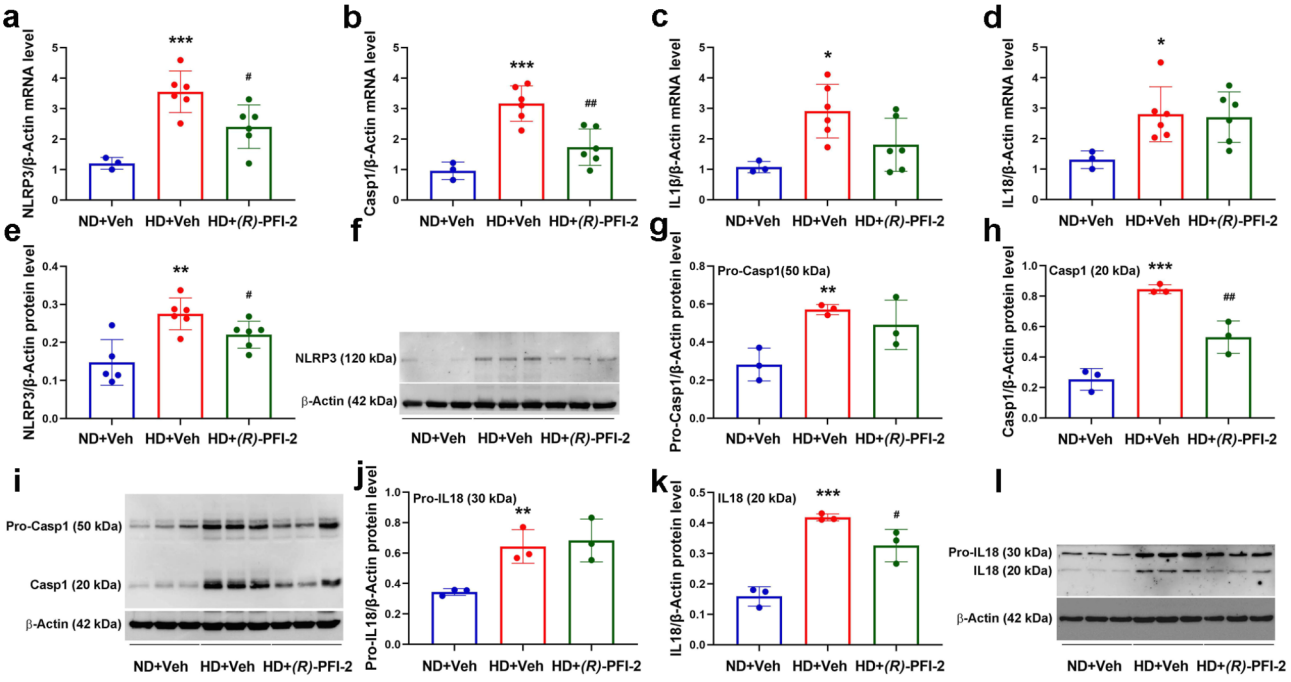

Fig. 5 SET7 mediates the upregulation of NLRP3 gene and protein expression in the atherosclerotic aorta of ApoE-/- mice. **a-d**, Gene expression analysis depicting the impact of SET7-oriented pharmacological intervention on NLRP3, Casp1, IL1β, and IL18 mRNA levels in the aortas. **e**, Downregulation of aortic NLRP3 protein level in atherosclerotic mice in response to (*R*)-PFI-2 intervention. **f**, Representative immunoblot showing the immunodetection of NLRP3 protein. **g-h**, Western blot analysis of pro-Casp1 (50 kDa) and Casp1 (20 kDa) activation status in the aortas. **i**, Representative immunoblot showing the zymogen form of Casp1 (Pro-Casp1) and its cleaved active form (Casp1). **j-k**, Western blot analysis of pro-IL18 (30 kDa) and active IL18 (20 kDa) level in the aorta of mice. **l**, Representative immunoblot presenting the IL18 precursor (Pro-IL18) and its active cleaved form (IL18). $n = 3–6$, * $p < 0.05$, *** $p < 0.001$. *p*-values were considered in relation to ND + Veh condition. # $p < 0.05$, ## $p < 0.01$. *p*-values were considered in relation to HD + Veh condition

SET7 mediates transcriptional up-regulation of Nox catalytic subunits and NLRP3 in pro-inflammatory macrophages

To investigate the potential involvement of SET7 in mediating the up-regulation of Nox subunit and NLRP3 inflammasome gene expression, M0, M1 and M2-polarized Mac were subjected to (*R*)-PFI-2 pharmacological intervention. We detected in M1-Mac as compared with M0-Mac (controls), significantly higher mRNA expression levels of Nox catalytic subunits, namely, Nox1 (≈3-fold), Nox2 (≈2.5-fold), Nox4 (≈5-fold), and Nox5 (≈4-fold), including p22phox (≈2-fold) essential subunit. Likewise, enhanced NLRP3 (≈3.5-fold), Casp1 (≈2.5-fold), IL1β (≈2.5-fold) and IL18 (≈6-fold) transcript levels were found in M1-Mac. In each case, blockade of SET7 catalytic activity suppressed the transcriptional up-regulation on Nox subunits, NLRP3, Casp1, IL1β, and IL-8 in M1-Mac (Fig. 7a-i).

To further ascertain the regulatory role of SET7 on Nox and NLRP3 gene expression we employed sinefungin, a potent SET7 pharmacological inhibitor. Sinefungin intervention mitigated the mRNA expression levels of Nox catalytic components, NLRP3, Casp1, IL1β, and IL-8 in M1-Mac (Figure S5). To complement the classical M1-Mac polarization procedure (employing LPS and IFNγ), cultured human Mac were challenged with oxLDL to induce a pro-inflammatory M1 phenotype, an atherosclerosis-relevant in vitro experimental set-up. Exposure of Mac to oxLDL induced marked increases in Nox catalytic subunit mRNA levels along with transcriptional up-regulation of NLRP3, Casp1, IL1β, and IL18. Of note, inhibition of SET7 catalytic activity suppressed oxLDL-induced gene expression of Nox subunits and NLRP3, Casp1, and IL18 in Mac (Figure S6).

To determine whether a similar regulatory pattern of SET7, Nox components, and NLRP3 expression also occurs in mouse Mac under pro-inflammatory conditions, we perform gene expression studies on cultured M1/M2-Mac derived from freshly isolated mouse Mon. Significant increases in SET7, Nox catalytic subunits, NLRP3, Casp1, IL1β, and IL18 mRNA levels were determined in cultured M1-Mac as compared to M0-Mac condition. The SET7 pharmacological inhibitor (*R*)-PFI-2 reduced the stimulatory effects on Nox subtypes and NLRP3 expression in M1-Mac, supporting our in-vivo findings in ApoE-/- mice and complements the results obtained on cultured human Mac (Fig. 7j-r).

Although the main focus of this study is to unveil the potential mechanistic link between SET7 and Nox, the contribution of other sources of ROS (e.g., mitochondria)

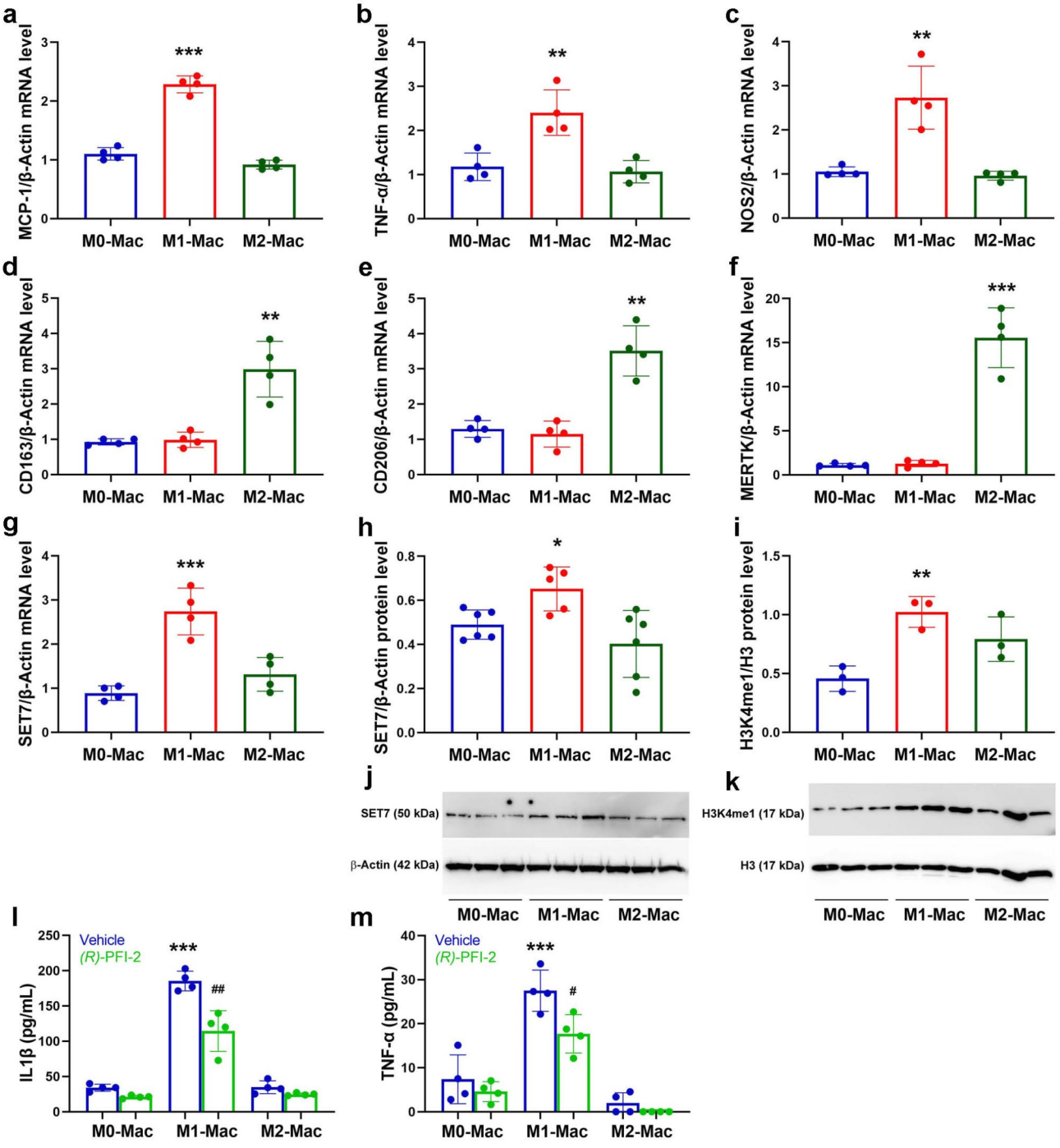

Fig. 6 Up-regulated SET7 expression and H3K4me1 level are associated with a Mac pro-inflammatory phenotype. **a-f**, Gene expression profiling of markers defining a pro-inflammatory M1-Mac (MCP-1, TNFα, NOS2) and anti-inflammatory M2-Mac (CD163, CD206, MERTK). **g**, Real-time PCR analysis depicting the up-regulation of SET7 transcript in M1-Mac. **h**, Western blot-related densitometric assessment showing the augmented SET7 relative protein level in cultured M1-Mac. **i**, Western blot quantification of H3K4me1 level is M0-Mac and in M1/M2-Mac. **j-k**, Representative blots showing the immunodetection of SET7 or H3K4me1 level in cell homogenates derived from M0-Mac and in vitro polarized M1/M2-Mac. **l-m**, Pharmacological inhibition of SET7 reduces IL1β and TNFα secretion in human M1-Mac. $n = 3–6$, * $p < 0.05$, ** $p < 0.01$, *** $p < 0.001$. p-values were considered in relation to M0-Mac condition. # $p < 0.05$, ## $p < 0.01$. p-values were considered in relation to vehicle-treated M1-Mac

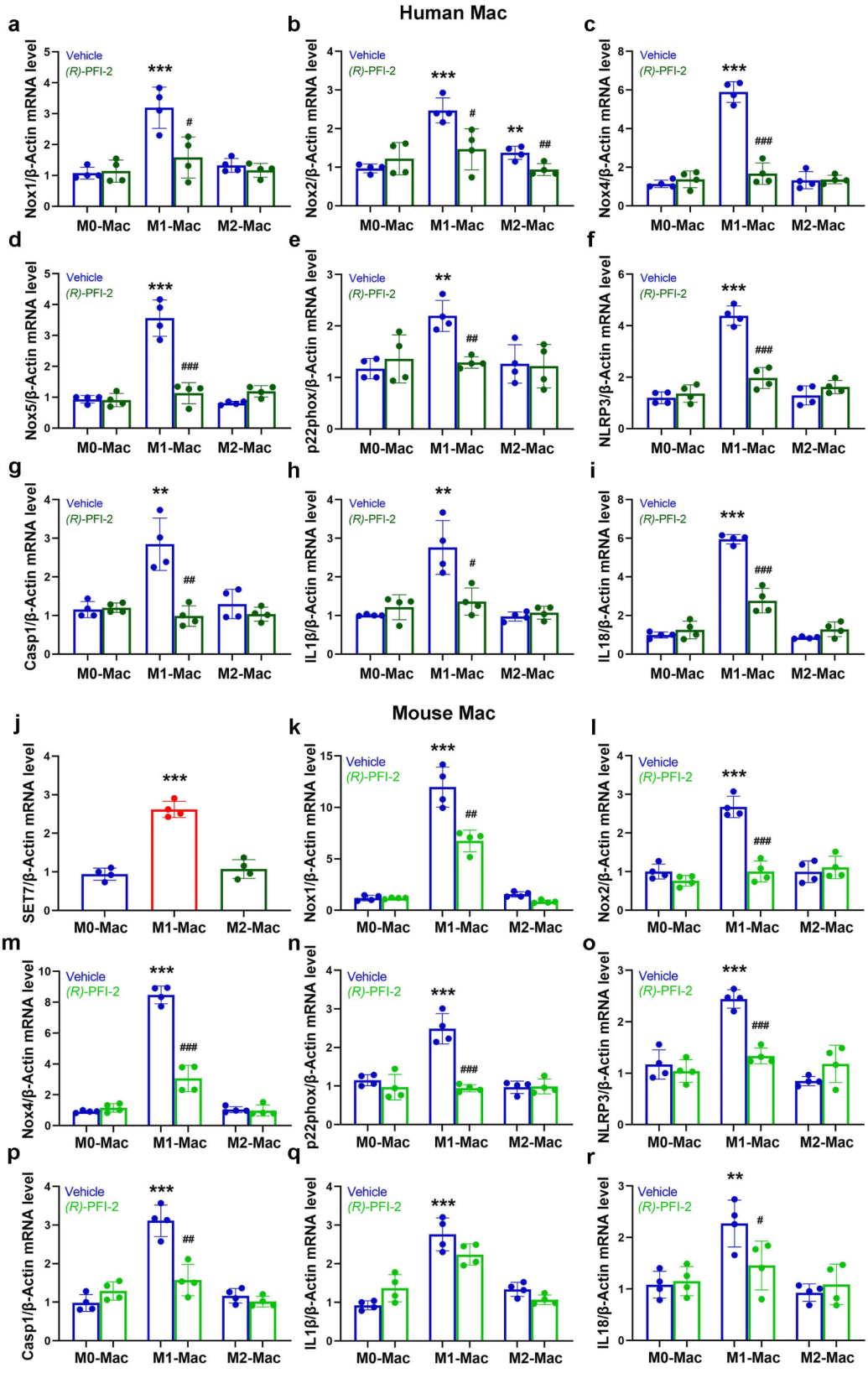

Fig. 7 (See legend on next page.)

(See figure on previous page.)

Fig. 7 SET7 mediates transcriptional up-regulation of Nox catalytic subunits and NLRP3 inflammasome in cultured human and mouse M1-Mac. **a-i**, Gene expression profiling of Nox1, Nox2, Nox4, Nox5, p22phox, NLRP3, Casp1, IL1β, and IL18 in Mac. **j**, Relative gene expression level of SET7 in resting (M0) and M1/M2-polarized mouse Mac. **k-r**, Nox1, Nox2, Nox4, p22phox, NLRP3, Casp1, IL1β, and IL18 gene expression analysis. $n = 4$, ** $p < 0.01$, *** $p < 0.001$. *p*-values were considered in relation to vehicle-exposed M0-Mac. # $p < 0.05$, ## $p < 0.01$, ### $p < 0.001$. *p*-values were considered in relation to vehicle-treated M1-Mac

to the overall oxidative insult in atherosclerosis should not be excluded. To further address this issue, we performed gene expression studies in cultured mouse M1/M2-Mac. Reportedly, succinate dehydrogenase (SDH) is a major source of ROS in response to inflammatory insults. We determined that the induction of SDHB and SDHD mRNA levels in cultured M1-Mac is partially mediated by SET7, as demonstrated by the inhibitory effects of (*R*)-PFI-2 pharmacological intervention. Interestingly, the up-regulated mitochondrial superoxide dismutase (SOD2) gene in M1-Mac was slightly attenuated in response to SET7 inhibition (Figure S7).

Collectively, the data advocate for the functional inference of SET7 with transcriptional programs that drive the up-regulation of Nox expression and key inflammation-related genes in Mac under the pro-inflammatory milieu of atherosclerosis.

Overexpression of SET7 triggers the up-regulation of Nox catalytic subunit transcript levels in EA.hy926 and HEK293 reporter cells

As indicated above, up-regulated SET7 expression is associated with advanced atherosclerotic lesions in human and mouse atherosclerotic arterial tissues and M1-Mac phenotype, and contributes to up-regulation of Nox expression, as revealed by the inhibitory effects of (*R*)-PFI-2 pharmacological compound. To further examine whether SET7 up-regulation has a direct impact on Nox subunit transcription we performed transfection assays. Although, M1/M2-polarized Mac is an important in vitro model of investigating both pro-inflammatory and anti-inflammatory aspects associated with atherosclerosis, Mac are notoriously difficult to transfect cells. Thus, to further examine whether SET7 up-regulation has a direct impact on Nox subunit transcription we performed transfection assays employing two different reporter cells, namely EA.hy926 and HEK293. In particular, HEK293 cells have been widely used to investigate different regulatory mechanisms of Nox expression and activation [38].

We detected a robust up-regulation of SET7 mRNA expression and protein level in pCMV6-SET7-transfected EA.hy926 cells when compared with controls, i.e. cells transfected with pCMV6-Entry empty vector. Overexpression of SET7 induced significant increases in Nox1 (≈3-fold), Nox2 (≈4-fold), Nox4 (≈2-fold), Nox5 (≈5-fold), and p22phox (≈5-fold) transcript levels. In addition, significant increases in NOS2, E-selectin, ICAM-1, and VCAM-1 mRNA levels, important markers of endothelial dysfunction and vascular inflammation, were determined in EA.hy926 overexpressing SET7 (Fig. 8). A similar regulatory pattern of Nox subunit transcriptional up-regulation was determined in SET7-transfected HEK293 cells (Figure S8). These findings suggest a direct mechanistic connection between up-regulated SET7 expression and enhanced Nox catalytic subunit transcription as well as selective inflammation-related genes associated with endothelial dysfunction and atherosclerosis.

Discussion

Despite adequate life style changes and standard therapeutic interventions, the patients with atherosclerotic disease have an increased risk of major adverse cardiovascular events (MACE) by pathological mechanisms that remain incompletely understood [39]. Hence, the development of more elaborated, potentially personalized, therapeutic strategies integrating highly specific pharmacological approaches and patient clinical characteristics are needed to efficiently reduce the incidence of atherosclerotic disease and its associated complications [14].

In recent years, an increasingly number of compelling clinical and experimental evidence indicates that the dysregulation of specific epigenetic mechanisms is functionally implicated in the pathoetiology of cardiometabolic disorders, including atherosclerosis [16, 40]. In particular, alterations in histone methylation-based regulatory mechanisms have been demonstrated to mediate both short-, and long-term transcriptional responses reflected in persistent activation of pro-oxidant and inflammation-related genes in various experimental models of CVD [41, 42].

Among other histone methyltransferases, SET7-induced adverse epigenetic changes and the consequent transcriptomic alterations have been associated with amplified inflammatory response, metabolic reprogramming, and trained immunity [43]. Noteworthy, these mechanistic processes are of particular importance for atherosclerotic plaque formation and destabilization [44, 45]. Yet, the precise role of SET7 in atherogenesis is not completely elucidated. In this context, we aimed to uncover whether SET7-induced epigenetic changes contribute to enhanced Nox subunit expression and NLRP3 inflammasome transcription and activation, key pathological processes contributing to ROS overproduction

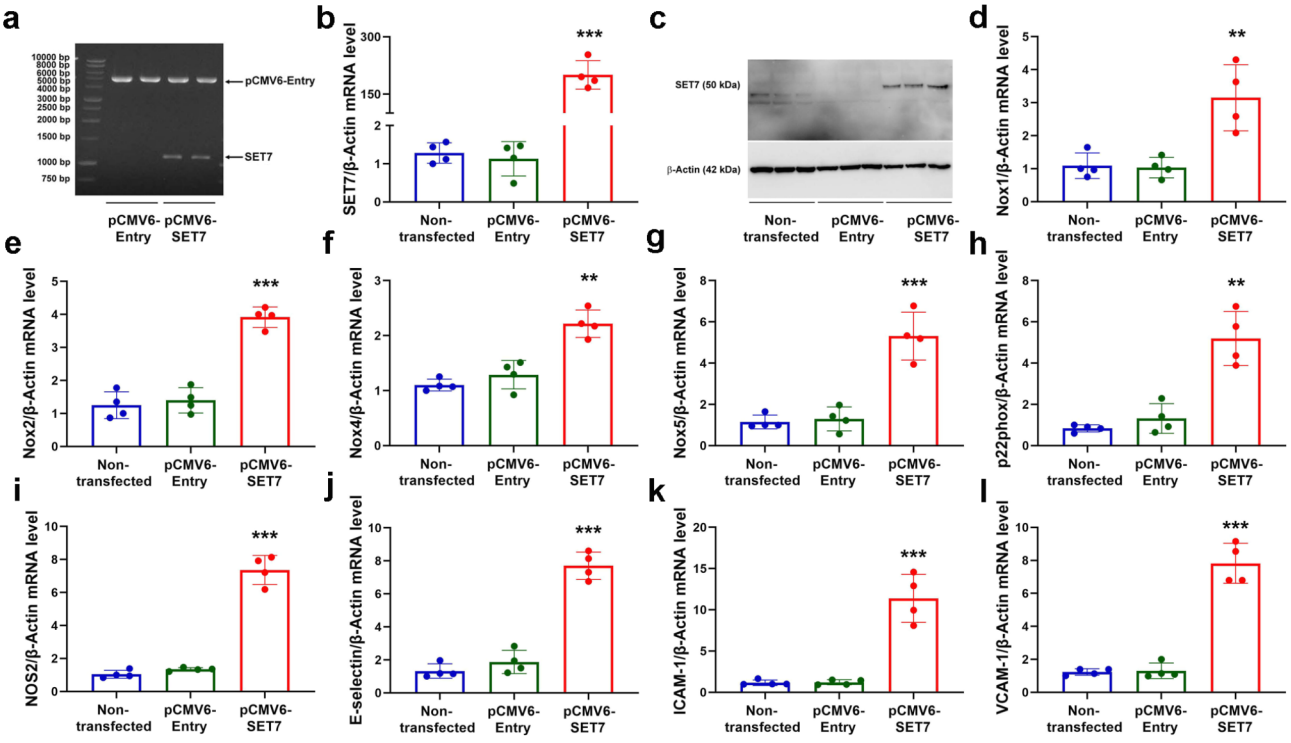

Fig. 8 Overexpression of SET7 promotes the up-regulation of Nox catalytic subunit mRNA levels in EA.hy926 cells. **a**, Representative image of a agarose gel electrophoresis (1%) showing the enzymatic digestion (SgfI/MluI) products of the pCMV6-Entry and pCMV6-SET7 plasmids. **b**, Validation of SET7 mRNA overexpression in pCMV6-SET7-transfected cells. **c**, Representative immunoblot depicting the augmented SET7 protein level in pCMV6-SET7-transfected cells. **d-i**, Gene expression analysis indicating transcriptional activation of Nox1, Nox2, Nox4, Nox5, p22phox, NOS2, E-selectin, ICAM-1, and VCAM-1 in EA.hy926 cells overexpressing SET7. $n = 4$, ** $p < 0.01$, *** $p < 0.001$. p-values were considered in relation to pCMV-6 Entry condition

and robust pro-inflammatory cytokine release in atherosclerosis.

Here, we report that SET7 mRNA and protein expression are up-regulated in human carotid atherosclerotic lesions and in the aorta of ApoE-/- mice with established atherosclerosis. Interestingly, recent genome-wide transcriptomic studies and bioinformatics analysis of public accessible microarray and RNA-sequencing data sets of human and mouse vascular disorders have revealed that SET7 is an important regulator of key innate immune genes linked to atherosclerotic plaque development [46]. Moreover, enhanced SET7 expression mediating persistent pro-inflammatory gene expression was reported in high glucose-exposed human endothelial cells and in monocytes derived from patients with type 2 diabetes [47, 48]. Since diabetes triggers endothelial dysfunction and monocyte commitment toward a pro-inflammatory phenotype, we may assume that SET7 could regulate important genes and pathways implicated in atherosclerotic lesion development.

To investigate the potential contribution of SET7 in atherogenesis, we used a highly selective pharmacological inhibitor developed by Pfizer, namely, (*R*)-PFI-2 [29] and ApoE-/- mice subjected to high-fat dietary intervention, as experimental model of atherosclerosis. We found that long-term blockade of SET7 catalytic function reduces the formation of atherosclerotic lesions in mice, irrespective of increased plasma total cholesterol and triglyceride levels. This observation offers an important clinical perspective for SET7-targeted pharmacological therapies as supportive strategy in reducing the burden of atherosclerosis-related CVD. Nevertheless, the results should be viewed in the context of ApoE-/- mouse model limitations that recapitulates to some extent important phenotypic aspects and processes resembling human atherosclerosis [28].

Among other dysregulated processes, excess formation of ROS driven by up-regulated Nox enzymes contributes to atherosclerotic plaque formation and stability. Previous compelling studies demonstrated that pharmacological inhibition or genetic ablation of different Nox subtypes is associated with reduced atherosclerotic lesion progression in mice [32, 49]. Other than direct targeting of specific Nox subtype function, pharmacological modulation of specific signalling mechanisms contributing to Nox up-regulation expression and/or activation has been also proposed [13, 50]. In the line with the latter concept, our study demonstrates that SET7 mediates the up-regulation of Nox1, Nox2, Nox4, and p22phox mRNA and protein expression levels in the atherosclerotic

aorta of mice, as indicated by the inhibitory effects of (*R*)-PFI-2 pharmacological compound. Our data are in a good agreement with a previous study demonstrating that silencing of SET7 in human aortic endothelial cells (EC) suppresses the high glucose-induced mRNA expression levels of oxidative stress-associated genes COX-2 and NOS2, and inflammation-related genes ICAM-1 and MCP-1, by a mechanism involving reduced p65/NF-kB subunit expression [48]. Similarly, SET7 has been shown to mediate NOS2 up-regulation in beta cells exposed to pro-inflammatory cytokines [51]. Consistent with these findings, our study provides new evidence that blockade of SET7 catalytic activity prevents the up-regulation of NOS2 gene and protein expression in the atherosclerotic aorta of mice. These are important observations that further strengthen the implication of SET7 signalling in mediating oxidant and inflammatory response in atherosclerosis. Noteworthy, it has been previously demonstrated that Nox4 has a protective function in the vasculature in specific pathological states [52]. Thus, considering these important findings, the downregulation of Nox4 expression in response to SET7 blockade could be viewed as potential side effect that should be considered.

Multiple histone-modifying enzymes regulating the status of histone acetylation (e.g., p300/CBP, HDAC1/2) and methylation (e.g., KDM1A, DOT1L, KMT5A) within specific gene enhancer and promoter regulatory regions have been proposed to play a role in atherogenesis [20, 22, 53–56]. We have previously demonstrated that p300/CBP, HDAC1/2 and KDM1A epigenetic enzymes are up-regulated in human and experimental atherosclerosis, and contribute to enhanced Nox subunit expression, oxidative stress, and inflammatory response in atherosclerotic mice [52, 55, 56]. These data suggest that a complex functional networking among multiple histone acetylation marks (i.e., H3K27ac, H3K9ac) regulating chromatin accessibility and combinatorial readout of specific histone methylation marks targeting enhancer/promoter regions are likely to be involved in the process of Nox subunit transcription. Noteworthy, other than histone proteins, additional molecular substrates of SET7 include inflammation-related transcription factors, namely, p65/NF-kB [57] and STAT3 [58]. Activation of SET7 has been demonstrated to enhance NF-kB signalling by two different cooperative mechanisms involving the up-regulation of p65/NF-kB expression, by direct H3K4me1 gene promoter interaction [48], and transcription factor activity, via methylation of K37 on p65/NF-kB [57]. Reportedly, SET7 methylates and inactivates STAT3, whereas KDM1A/LSD1 demethylates and activates STAT3 [58]. Since both SET7 and KDM1A/LSD1 are up-regulated in atherosclerosis, we may safely assume that, function on the pathophysiological context, histone-dependent and histone-independent cooperative mechanisms fine-tune the expression of specific inflammation-associated genes. Of note, there is evidence that NF-kB and STAT3 are key transcriptional regulators of various Nox subtypes in vascular smooth muscle cells and macrophages exposed to pro-inflammatory conditions [59–61]. In addition, SET7 contributes to protein synthesis by methylation of ribosomal protein eL42 [27]. Thus, we may presume that SET7 may induce pleiotropic regulatory effects in atherosclerosis leading to augmented Nox expression via histone marks and transcription factors enrichment at the sites of Nox gene enhancers and promoters, and potentially enhanced Nox subtype protein synthesis via ribosomal subunit eL42 methylation.

Elevated Nox expression has been increasingly associated with ROS overproduction in different experimental settings, suggesting a direct correlation between the relative abundance of Nox subunits and Nox enzymatic activity. Yet, measurement of the rate of ROS formation in isolated cells and tissues raises certain technical challenges, mainly related to the specificity of the redox-sensitive probes. In addition, most assays do not reflect the complexity of the processes characterizing physiological or specific pathophysiological conditions but rather the potential of a biological sample to produce ROS under control laboratory conditions [62]. In this context, analysis of more stable chemical modifications of proteins, lipids, and nucleic acids produced under oxidant milieu emerged as an important strategy to assess oxidative stress [63]. Given these important aspects, in this study we analyzed the formation of two different markers, namely, NT- and 4HNE-protein adducts, to estimate the overall extent of vascular oxidative stress in atherosclerotic mice. We determined that SET7 blockade attenuates the formation of NT- and 4HNE-modified proteins in the aorta of atherosclerotic mice. Our findings suggest that activation of SET7 signalling positively interferes with mechanisms of ROS overproduction in atherosclerosis. Since Nox-derived ROS are important triggers of NT and 4HNE formation, we may speculate that NT- and 4HNE-induced protein modifications in the aorta of atherosclerotic mice are partially related to the up-regulated Nox. Hence, the contribution of other enzymatic and non-enzymatic sources of ROS mediating these effects should be considered.

In view of the multifactorial nature of atherosclerosis, the excess formation of ROS, potentially triggered by up-regulated Nox, represents just one important aspect of this complex vascular disorder. Since oxidative stress and inflammation are functionally interconnected in atherogenesis, we questioned whether SET7 plays a role in mediating the inflammatory response in atherosclerosis, in addition to regulating the mechanisms of ROS formation. We focused on NLRP3 inflammasome system considering its instrumental role in the process of

atheroma formation [64, 65]. Employing a highly specific pharmacological intervention we found that SET7 contributes to NLRP3 up-regulation, leading enhanced pro-Casp-1 and pro-IL18 cleavage in the atherosclerotic aorta of mice. This important observation could further explain the impact of SET7 blockade on atherosclerotic lesion progression in mice. Noteworthy, NLRP3 inflammasome priming and activation are critical consequences of the oxidant milieu in atherosclerosis. In this context, Nox-derived ROS have been mechanistically implicated in NLRP3 inflammasome priming via redox-sensitive NF-kB transcription factor activation. ROS produced by activated Nox may also act as triggers of NLRP3 inflammasome activation [35]. Yet, considering the current status of knowledge in the field, multiple sources of ROS (e.g., mitochondria), as well as redox-independent mechanisms should be considered as potential signals leading to NLRP3 inflammasome activation and pro-inflammatory cytokine production in atherogenesis.

To further investigate the implication of SET7 in atherosclerosis, we complemented the in vivo studies with in vitro experiments on human and mouse Mac that play major roles in all inflammatory phases of plaque development [65]. Apart from this, Mac typically express functional Nox subtypes and NLRP3 inflammasome components, and consequently they are a reliable model to examine SET7-related transcriptional regulatory mechanisms [66, 67]. Nevertheless, the contribution of SET7 in other cell types and their functional cross-communications in atherosclerotic lesion development should not be underestimated.

Evidence exists that SET7 expression is induced in human Mac under pro-inflammatory conditions and is typically correlated with enhanced H3K4me1 level at specific sites within the regulatory elements of inflammation and citric acid cycle genes, leading to a persistent pro-inflammatory Mac phenotype. In addition, activation of SET7 promotes long-lasting epigenetic imprints characteristically associated with trained immunity, a process that could explain the sustained hyperactivity of innate immune cells and the recurrent MACE in atherosclerotic patients [22, 44, 48]. Our data are in a good agreement and extend these observations. Employing a standard in vitro Mac polarization protocol, we determined that enhanced SET7 expression and augmented H3K4me1 level are associated with a pro-inflammatory M1-Mac phenotype. Moreover, we found that blockade of SET7 function suppresses the transcription of Nox catalytic subunits and NLRP3 inflammasome in M1-Mac. Noteworthy, Mac polarization toward a M1-, or M2-Mac phenotype has been extensively employed to uncover the molecular and functional characteristics and specific pro-inflammatory/ anti-inflammatory role in plaque formation [55]. However, the combined stimulatory effects of LPS and IFNγ in inducing M1-Mac phenotype may not accurately reflect the phenotypic characteristics of Mac implicated in atheroma formation. Thus, as an additional atherosclerosis-relevant in vitro experimental set-up and to further validate our findings, cultured human Mac were challenged with oxLDL. Of note, SET7 pharmacological intervention prevented the up-regulation of Nox catalytic subunit and NLPR3 mRNA expression in oxLDL-stimulated human Mac. These results indicate that activation of SET7 signalling is likely to induce transcriptional programs in Mac with consequences on plaque formation, namely the oxidative stress and inflammation.

Complex functional interactions and highly dynamic networking among multiple pathological processes define the atherosclerotic plaque phenotype. Of these, increased formation of Nox-derived ROS and enhanced pro-inflammatory cytokine production are important, but note the sole contributors to atherosclerotic plaque formation. Consequently, in addition to Nox and NLRP3, the potential impact of SET7 on other atherosclerosis-relevant genes and pathways remains to be further elucidated. Open issues include but not limited to the role of SET7 in metabolic reprogramming and phenotypic alterations of vascular cells and immune cells, extracellular matrix remodelling, pathways associated with cholesterol transport and foam cell formation, as well as other sources of ROS production in atherosclerosis.

Although several phenotypic and mechanistic similarities of atherosclerotic lesion development and progression in humans and mice exist [28], the findings of this study should be viewed in the context of animal model limitation to accurately reflect the complex pathology of human atherosclerotic disease.

To investigate the potential implication of SET7 in mediating the up-regulation of Nox and NLRP3 expression in experimental atherosclerosis, we used (*R*)-PFI-2, a highly specific pharmacological inhibitor. Even though (*R*)-PFI-2 pharmacological compound is currently the most potent and selective inhibitor of SET7 catalytic activity [29], our findings are not supported by experiments employing knockout or knockdown molecular interventions. These are important aspects that should be further considered in view of further clinical development and implementation of SET7-specific pharmacological interventions, as supportive therapeutic strategy to mitigate oxidative stress and inflammation in atherosclerosis.

Conclusions

Collectively, our in vivo and in vitro experimental models, provide novel evidence that SET7 function as a molecular hub controlling the transcription of key pro-oxidant (i.e., Nox enzymes) and pro-inflammatory (i.e.,

NLRP3 inflammasome) genes that are mechanistically related to atherogenesis. The data suggest that SET7 may become a new pharmacological target in atherosclerotic cardiovascular disease.

Abbreviations

SET7	SET domain containing 7 histone lysine methyltransferase
ROS	Reactive oxygen species
NADPH	Nicotinamide adenine dinucleotide phosphate (reduced form)
Nox	NADPH oxidase
NOS2	Nitric oxide synthase 2
CVD	Cardiovascular disorders
LPS	Lipopolizaharide
IFNγ	Interferon gamma
IL-4	Interleukin-4
IL-13	Interleukin-13
NLRP3	NLR family pyrin domain containing 3
Casp1	caspase 1
IL1β	Interleukin-1β
IL18	Interleukin-18
MCP-1	Monocyte chemoattractant protein-1
TNFα	tumor necrosis factorα
CD163	Cluster of differentiation 163
CD206	Cluster of differentiation 206/manose receptor
MERTK	Proto-oncogene tyrosine-protein kinase MER
H3	histone H3
ICAM-1	Intercellular Adhesion Molecule 1
VCAM-1	Vascular Cell Adhesion Molecule 1
NF-kB	Nuclear factor kappa-light-chain-enhancer of activated B cells
STAT	Signal transducer and activator of transcription
LDL	Low-density lipoprotein
HDL	High-density lipoprotein
EDTA	Ethylenediaminetetraacetic acid disodium salt dehydrate
SDS-PAGE	Sodium dodecyl sulfate-polyacrylamide gel electrophoresis
DMSO	Dimethyl sulfoxide
PBS	Phosphate-buffered saline
RIPA	Radioimmunoprecipitation assay buffer

Supplementary Information

The online version contains supplementary material available at https://doi.org/10.1186/s12967-025-06338-0.

Supplementary Material 1

Acknowledgements

The authors are thankful to Nae Sanda and Constanta Stan for their helpful technical assistance.

Author contributions

Simona-Adriana Manea, Mihaela-Loredana Vlad, Adrian Manea: the conception and design of the study; acquisition of data; analysis and interpretation of data; drafting the article and revising it critically for important intellectual content. Alexandra-Gela Lazar: data acquisition, analysis and interpretation of data; Horia Muresian: collection of biological samples, analysis and interpretation of data; drafting the article; revising it critically for important intellectual content. Maya Simionescu: drafting the article; revising it critically for important intellectual content.

Funding

This work was supported by Romanian Academy and grants from the Ministry of Research, Innovation and Digitization, CNCS– UEFISCDI (project number PN-III-P4-ID-PCE-2020-1898 (Contract number PCE81/2021), project number PN-III-P1-1.1-TE-2021-0180 (Contract number TE141/2022)), within PNCDI III, and Romania's National Recovery and Resilience Plan, PNRR-III-C9-2022-I8, CF148/15.11.2022, Financing Contract no. 760061/23.05.2023.

Data availability

The datasets used and/or analysed during the current study are available from the corresponding author on reasonable request.

Declarations

Ethics approval and consent to participate

The study was done in agreement with the ethical directives for medical research implicating human subjects (The Code of Ethics of the World Medical Association, Declaration of Helsinki). Written informed consent was provided by the study patients. The experimental protocols were approved by the ethical committee of the Institute of Cellular Biology and Pathology (ICBP) "Nicolae Simionescu" (#11/29.06.2016, #03/07.04.2021). Animal study protocols conformed to the guidelines of EU Directive 2010/63/EU, and were approved by the ethical committee of the ICBP "Nicolae Simionescu" (#04/07.04.2021).

Consent for publication

Not applicable.

Competing interests

The authors declare that they have no competing interests.

Author details

[1]Institute of Cellular Biology and Pathology "Nicolae Simionescu" of the Romanian Academy, 8, B.P. Hasdeu Street, Bucharest 050568, Romania
[2]Cardiovascular Surgery Department, University Hospital Bucharest, Bucharest, Romania

Received: 12 August 2024 / Accepted: 1 March 2025
Published online: 17 March 2025

References

1. Förstermann U, Xia N, Li H. Roles of vascular oxidative stress and nitric oxide in the pathogenesis of atherosclerosis. Circ Res. 2017;120(4):713–35. https://doi.org/10.1161/CIRCRESAHA.116.309326.
2. Yuan T, Yang T, Chen H, Fu D, Hu Y, Wang J, Yuan Q, Yu H, Xu W, Xie X. New insights into oxidative stress and inflammation during diabetes mellitus-accelerated atherosclerosis. Redox Biol. 2019;20:247–60. https://doi.org/10.1016/j.redox.2018.09.025.
3. Marchio P, Guerra-Ojeda S, Vila JM, Aldasoro M, Victor VM, Mauricio MD. Targeting early atherosclerosis: a focus on oxidative stress and inflammation. Oxid Med Cell Longev. 2019;2019:8563845. https://doi.org/10.1155/2019/8563845.
4. Zhang Y, Murugesan P, Huang K, Cai H. NADPH oxidases and oxidase crosstalk in cardiovascular diseases: novel therapeutic targets. Nat Rev Cardiol. 2020;17(3):170–94. https://doi.org/10.1038/s41569-019-0260-8.
5. Yan R, Zhang X, Xu W, Li J, Sun Y, Cui S, Xu R, Li W, Jiao L, Wang T. ROS-induced endothelial dysfunction in the pathogenesis of atherosclerosis. Aging Dis. 2024. https://doi.org/10.14336/AD.2024.0309.
6. Frey RS, Ushio-Fukai M, Malik AB. NADPH oxidase-dependent signaling in endothelial cells: role in physiology and pathophysiology. Antioxid Redox Signal. 2009;11(4):791–810. https://doi.org/10.1089/ars.2008.2220.
7. Marqués J, Cortés A, Pejenaute Á, Zalba G. Implications of NADPH oxidase 5 in vascular diseases. Int J Biochem Cell Biol. 2020;128:105851. https://doi.org/10.1016/j.biocel.2020.105851.
8. Poznyak AV, Grechko AV, Orekhova VA, Khotina V, Ivanova EA, Orekhov AN. NADPH oxidases and their role in atherosclerosis. Biomedicines. 2020;8(7):206. https://doi.org/10.3390/biomedicines8070206.
9. Drummond GR, Selemidis S, Griendling KK, Sobey CG. Combating oxidative stress in vascular disease: NADPH oxidases as therapeutic targets. Nat Rev Drug Discov. 2011;10(6):453–71. https://doi.org/10.1038/nrd3403.
10. Gray SP, Jandeleit-Dahm KA. The role of NADPH oxidase in vascular disease-hypertension, atherosclerosis & stroke. Curr Pharm Des. 2015;21(41):5933–44. https://doi.org/10.2174/1381612821666151029112302.
11. Aguado A, Fischer T, Rodríguez C, Manea A, Martínez-González J, Touyz RM, Hernanz R, Alonso MJ, Dixon DA, Briones AM, Salaices M. Hu antigen R is required for NOX-1 but not NOX-4 regulation by inflammatory stimuli in vascular smooth muscle cells. J Hypertens. 2016;34(2):253–65. https://doi.org/10.1097/HJH.0000000000000801.

12. Vermot A, Petit-Härtlein I, Smith SME, Fieschi F. NADPH oxidases (NOX): an overview from discovery, molecular mechanisms to physiology and pathology. Antioxid (Basel). 2021;10(6):890. https://doi.org/10.3390/antiox10060890.
13. Manea SA, Constantin A, Manda G, Sasson S, Manea A. Regulation of Nox enzymes expression in vascular pathophysiology: focusing on transcription factors and epigenetic mechanisms. Redox Biol. 2015;5:358–66. https://doi.org/10.1016/j.redox.2015.06.012.
14. Costantino S, Libby P, Kishore R, Tardif JC, El-Osta A, Paneni F. Epigenetics and precision medicine in cardiovascular patients: from basic concepts to the clinical arena. Eur Heart J. 2018;39(47):4150–8. https://doi.org/10.1093/eurheartj/ehx568.
15. Wang Y, Miao X, Liu Y, Li F, Liu Q, Sun J, Cai L. Dysregulation of histone acetyltransferases and deacetylases in cardiovascular diseases. Oxid Med Cell Longev. 2014;2014:641979. https://doi.org/10.1155/2014/641979.
16. Herman AB, Occean JR, Sen P. Epigenetic dysregulation in cardiovascular aging and disease. J Cardiovasc Aging. 2021;1:10. https://doi.org/10.20517/jca.2021.16.
17. Musselman CA, Lalonde ME, Côté J, Kutateladze TG. Perceiving the epigenetic landscape through histone readers. Nat Struct Mol Biol. 2012;19(12):1218–27. https://doi.org/10.1038/nsmb.2436.
18. Morera L, Lübbert M, Jung M. Targeting histone methyltransferases and demethylases in clinical trials for cancer therapy. Clin Epigenetics. 2016;8:57. https://doi.org/10.1186/s13148-016-0223-4.
19. Greißel A, Culmes M, Burgkart R, Zimmermann A, Eckstein HH, Zernecke A, Pelisek J. Histone acetylation and methylation significantly change with severity of atherosclerosis in human carotid plaques. Cardiovasc Pathol. 2016;25(2):79–86. https://doi.org/10.1016/j.carpath.2015.11.001.
20. Farina FM, Serio S, Hall IF, Zani S, Cassanmagnago GA, Climent M, Civilini E, Condorelli G, Quintavalle M, Elia L. The epigenetic enzyme DOT1L orchestrates vascular smooth muscle cell-monocyte crosstalk and protects against atherosclerosis via the NF-kappaB pathway. Eur Heart J. 2022;43(43):4562–76. https://doi.org/10.1093/eurheartj/ehac097.
21. Willemsen L, Prange KHM, Neele AE, van Roomen CPAA, Gijbels M, Griffith GR, Toom MD, Beckers L, Siebeler R, Spann NJ, Chen HJ, Bosmans LA, Gorbatenko A, van Wouw S, Zelcer N, Jacobs H, van Leeuwen F, de Winther MPJ. DOT1L regulates lipid biosynthesis and inflammatory responses in macrophages and promotes atherosclerotic plaque stability. Cell Rep. 2022;41(8):111703. https://doi.org/10.1016/j.celrep.2022.111703.
22. Dong Z, Hou L, Luo W, Pan LH, Li X, Tan HP, Wu RD, Lu H, Yao K, Mu MD, Gao CS, Weng XY, Ge JB. Myocardial infarction drives trained immunity of monocytes, accelerating atherosclerosis. Eur Heart J. 2024;45(9):669–84. https://doi.org/10.1093/eurheartj/ehad787.
23. Keating ST, El-Osta A. Transcriptional regulation by the Set7 lysine methyltransferase. Epigenetics. 2013;8(4):361–72. https://doi.org/10.4161/epi.24234.
24. Batista IAA, Helguero LA. Biological processes and signal transduction pathways regulated by the protein methyltransferase SETD7 and their significance in cancer. Signal Transduct Target Ther. 2018;13:319. https://doi.org/10.1038/s41392-018-0017-6.
25. Gao L, Yu W, Song P, Li Q. Non-histone methylation of SET7/9 and its biological functions. Recent Pat Anticancer Drug Discov. 2022;17(3):231–43. https://doi.org/10.2174/1574892816666211202160041.
26. Li Y, Reddy MA, Miao F, Shanmugam N, Yee JK, Hawkins D, Ren B, Natarajan R. Role of the histone H3 lysine 4 methyltransferase, SET7/9, in the regulation of NF-kappaB-dependent inflammatory genes. Relevance to diabetes and inflammation. J Biol Chem. 2008;283(39):26771–81. https://doi.org/10.1074/jbc.M802800200.
27. Mahesh A, Khan MIK, Govindaraju G, Verma M, Awasthi S, Chavali PL, Chavali S, Rajavelu A, Dhayalan A. SET7/9 interacts and methylates the ribosomal protein, eL42 and regulates protein synthesis. Biochim Biophys Acta Mol Cell Res. 2020;1867(2):118611. https://doi.org/10.1016/j.bbamcr.2019.118611.
28. Nakashima Y, Plump AS, Raines, Breslow JL, Ross R. ApoE-deficient mice develop lesions of all phases of atherosclerosis throughout the arterial tree. Arterioscler Thromb Vasc Biol. 1994;14(1):133–40. https://doi.org/10.1161/01.atv.14.1.133.
29. Barsyte-Lovejoy D, Li F, Oudhoff MJ, Tatlock JH, Dong A, Zeng H, Wu H, Freeman SA, Schapira M, Senisterra GA, Kuznetsova E, Marcellus R, Allali-Hassani A, Kennedy S, Lambert JP, Couzens AL, Aman A, Gingras AC, Al-Awar R, Fish PV, Gerstenberger BS, Roberts L, Benn CL, Grimley RL, Braam MJS, Rossi FMV, Sudol M, Brown PJ, Bunnage ME, Owen DR, Zaph C, Vedadi M, Arrowsmith CH. (R)-PFI-2 is a potent and selective inhibitor of SETD7 methyltransferase activity in cells. Proc Natl Acad Sci U S A. 2014;111(35):12853–8. https://doi.org/10.1073/pnas.1407358111.
30. Manea A, Manea SA, Gan AM, Constantin A, Fenyo IM, Raicu M, Muresian H, Simionescu M. Human monocytes and macrophages express NADPH oxidase 5; a potential source of reactive oxygen species in atherosclerosis. Biochem Biophys Res Commun. 2015;461(1):172–9. https://doi.org/10.1016/j.bbrc.2015.04.021.
31. Pfaffl MW. A new mathematical model for relative quantification in real-time RT-PCR. Nucleic Acids Res. 2001;29(9):e45. https://doi.org/10.1093/nar/29.9.e45.
32. Gray SP, Jha JC, Kennedy K, van Bommel E, Chew P, Szyndralewiez C, Touyz RM, Schmidt HHHW, Cooper ME, Jandeleit-Dahm KAM. Combined NOX1/4 Inhibition with GKT137831 in mice provides dose-dependent reno- and atheroprotection even in established micro- and macrovascular disease. Diabetologia. 2017;60(5):927–37. https://doi.org/10.1007/s00125-017-4215-5.
33. Manea A, Simionescu M. Nox enzymes and oxidative stress in atherosclerosis. Front Biosci (Schol Ed). 2012;4(2):651–70. https://doi.org/10.2741/s291.
34. Steven S, Frenis K, Oelze M, Kalinovic S, Kuntic M, Bayo Jimenez MT, Vujacic-Mirski K, Helmstädter J, Kröller-Schön S, Münzel T, Daiber A. Vascular inflammation and oxidative stress: Major triggers for cardiovascular disease. Oxid Med Cell Longev. 2019;2019:7092151. https://doi.org/10.1155/2019/7092151
35. Abais JM, Xia M, Zhang Y, Boini KM, Li PL. Redox regulation of NLRP3 inflammasomes: ROS as trigger or effector? Antioxid Redox Signal. 2015;22(13):1111–29. https://doi.org/10.1089/ars.2014.5994.
36. McKee CM, Coll RC. NLRP3 inflammasome priming: A riddle wrapped in a mystery inside an enigma. J Leukoc Biol. 2020;108(3):937–52. https://doi.org/10.1002/JLB.3MR0720-513R.
37. Lu N, Cheng W, Liu D, Liu G, Cui C, Feng C, Wang X. NLRP3-mediated inflammation in atherosclerosis and associated therapeutics. Front Cell Dev Biol. 2022;10:823387. https://doi.org/10.3389/fcell.2022.823387.
38. Kawahara T, Ritsick D, Cheng G, Lambeth JD. Point mutations in the proline-rich region of p22phox are dominant inhibitors of Nox1- and Nox2-dependent reactive oxygen generation. J Biol Chem. 2005;280(36):31859–69. https://doi.org/10.1074/jbc.M501882200.
39. Timmis A, Townsend N, Gale CP, Torbica A, Lettino M, Petersen SE, Mossialos EA, Maggioni AP, Kazakiewicz D, May HT, De Smedt D, Flather M, Zuhlke L, Beltrame JF, Huculeci R, Tavazzi L, Hindricks G, Bax J, Casadei B, Achenbach S, Wright L, Vardas P. European society of cardiology. European society of cardiology. cardiovascular disease statistics 2019. Eur Heart J. 2020;41(1):12–85. https://doi.org/10.1093/eurheartj/ehz859.
40. Harman JL, Dobnikar L, Chappell J, Stokell BG, Dalby A, Foote K, Finigan A, Freire-Pritchett P, Taylor AL, Worssam MD, Madsen RR, Loche E, Uryga A, Bennett MR, Jørgensen HF. Epigenetic regulation of vascular smooth muscle cells by histone H3 lysine 9 dimethylation attenuates target gene-induction by inflammatory signaling. Arterioscler Thromb Vasc Biol. 2019;39(11):2289–302. https://doi.org/10.1161/ATVBAHA.119.312765.
41. Bekkering S, Quintin J, Joosten LAB, van der Meer JWM, Netea MG, Riksen NP. Oxidized low-density lipoprotein induces long-term Proinflammatory cytokine production and foam cell formation via epigenetic reprogramming of monocytes. Arterioscler Thromb Vasc Biol. 2014;34(8):1731–8. https://doi.org/10.1161/ATVBAHA.114.303887.
42. Yang Y, Luan Y, Yuan RX, Luan Y. Histone methylation related therapeutic challenge in cardiovascular diseases. Front Cardiovasc Med. 2021;8:710053. https://doi.org/10.3389/fcvm.2021.710053.
43. Keating ST, Groh L, van der Heijden CDCC, Rodriguez H, Dos Santos JC, Fanucchi S, Okabe J, Kaipananickal H, van Puffelen JH, Helder L, Noz MP, Matzaraki V, Li Y, de Bree LCJ, Koeken VACM, Moorlag SJCFM, Mourits VP, Domínguez-Andrés J, Oosting M, Bulthuis EP, Koopman WJH, Mhlanga M, El-Osta A, Joosten LAB, Netea MG, Riksen NP. The Set7 lysine methyltransferase regulates plasticity in oxidative phosphorylation necessary for trained immunity induced by beta-glucan. Cell Rep. 2020;31(3):107548. https://doi.org/10.1016/j.celrep.2020.107548.
44. Flores-Gomez D, Bekkering S, Netea MG, Riksen NP. Trained immunity in atherosclerotic cardiovascular disease. Arterioscler Thromb Vasc Biol. 2021;41(1):62–9. https://doi.org/10.1161/ATVBAHA.120.314216.
45. Riksen NP, Bekkering S, Mulder WJM, Netea MG. Trained immunity in atherosclerotic cardiovascular disease. Nat Rev Cardiol. 2023;20(12):799–811. https://doi.org/10.1038/s41569-023-00894-y.
46. Yang Q, Saaoud F, Lu Y, Pu Y, Xu K, Shao Y, Jiang X, Wu S, Yang L, Tian Y, Liu X, Gillespie A, Luo JJ, Shi XM, Zhao H, Martinez L, Vazquez-Padron R, Wang H, Yang X. Innate immunity of vascular smooth muscle cells contributes to two-wave inflammation in atherosclerosis, twin-peak inflammation in aortic aneurysms and trans-differentiation potential into 25 cell types. Front Immunol. 2024;14:1348238. https://doi.org/10.3389/fimmu.2023.1348238.

47. Okabe J, Orlowski C, Balcerczyk A, Tikellis C, Thomas MC, Cooper ME, El-Osta A. Distinguishing hyperglycemic changes by Set7 in vascular endothelial cells. Circ Res. 2012;110(8):1067–76. https://doi.org/10.1161/CIRCRESAHA.112.266171.
48. Paneni F, Costantino S, Battista R, Castello L, Capretti G, Chiandotto S, Scavone G, Villano A, Pitocco D, Lanza G, Volpe M, Lüscher TF, Cosentino F. Adverse epigenetic signatures by histone methyltransferase Set7 contribute to vascular dysfunction in patients with type 2 diabetes mellitus. Circ Cardiovasc Genet. 2015;8(1):150–8. https://doi.org/10.1161/CIRCGENETICS.114.000671.
49. Gray SP, Di Marco E, Okabe J, Szyndralewiez C, Heitz F, Montezano AC, de Haan JB, Koulis C, El-Osta A, Andrews KL, Chin-Dusting JPF, Touyz RM, Wingler K, Cooper ME, Schmidt HHHW, Jandeleit-Dahm KA. NADPH oxidase 1 plays a key role in diabetes mellitus-accelerated atherosclerosis. Circulation. 2013;127(18):1888–902. https://doi.org/10.1161/CIRCULATIONAHA.112.132159.
50. Manea SA, Todirita A, Raicu M, Manea A. C/EBP transcription factors regulate NADPH oxidase in human aortic smooth muscle cells. J Cell Mol Med. 2014;18(7):1467–77. https://doi.org/10.1111/jcmm.12289.
51. Fujimaki K, Ogihara T, Morris DL, Oda H, Iida H, Fujitani Y, Mirmira RG, Evans-Molina C, Watada H. SET7/9 enzyme regulates cytokine-induced expression of inducible nitric-oxide synthase through methylation of lysine 4 at histone 3 in the islet B cell. J Biol Chem. 2015;290(27):16607–18. https://doi.org/10.1074/jbc.M115.661777.
52. Schröder K, Zhang M, Benkhoff S, Mieth A, Pliquett R, Kosowski J, Kruse C, Luedike P, Michaelis UR, Weissmann N, Dimmeler S, Shah AM, Brandes RP. Nox4 is a protective reactive oxygen species generating vascular NADPH oxidase. Circ Res. 2012;110(9):1217–25. https://doi.org/10.1161/CIRCRESAHA.112.267054.
53. Vlad ML, Manea SA, Lazar AG, Raicu M, Muresian H, Simionescu M, Manea A. Histone acetyltransferase-dependent pathways mediate upregulation of NADPH oxidase 5 in human macrophages under inflammatory conditions: A potential mechanism of reactive oxygen species overproduction in atherosclerosis. Oxid Med Cell Longev. 2019;2019:3201062. https://doi.org/10.1155/2019/3201062
54. Manea SA, Antonescu ML, Fenyo IM, Raicu M, Simionescu M, Manea A. Epigenetic regulation of vascular NADPH oxidase expression and reactive oxygen species production by histone deacetylase-dependent mechanisms in experimental diabetes. Redox Biol. 2018;16:332–43. https://doi.org/10.1016/j.redox.2018.03.011.
55. Manea SA, Vlad ML, Fenyo IM, Lazar AG, Raicu M, Muresian H, Simionescu M, Manea A. Pharmacological Inhibition of histone deacetylase reduces NADPH oxidase expression, oxidative stress and the progression of atherosclerotic lesions in hypercholesterolemic Apolipoprotein E-deficient mice; potential implications for human atherosclerosis. Redox Biol. 2020;28:101338. https://doi.org/10.1016/j.redox.2019.101338.
56. Manea SA, Vlad ML, Lazar AG, Muresian H, Simionescu M, Manea A. Pharmacological Inhibition of lysine-specific demethylase 1A reduces atherosclerotic lesion formation in Apolipoprotein E-deficient mice by a mechanism involving decreased oxidative stress and inflammation; potential implications in human atherosclerosis. Antioxid (Basel). 2022;11(12):2382. https://doi.org/10.3390/antiox11122382.
57. Ea CK, Baltimore D. Regulation of NF-kappaB activity through lysine monomethylation of p65. Proc Natl Acad Sci U S A. 2009;106(45):18972–7. https://doi.org/10.1073/pnas.0910439106.
58. Yang J, Huang J, Dasgupta M, Sears N, Miyagi M, Wang B, Chance MR, Chen X, Du Y, Wang Y, An L, Wang Q, Lu T, Zhang X, Wang Z, Stark GR. Reversible methylation of promoter-bound STAT3 by histone-modifying enzymes. Proc Natl Acad Sci U S A. 2010;107(50):21499–504. https://doi.org/10.1073/pnas.1016147107.
59. Anrather J, Racchumi G, Iadecola C. NF-kappaB regulates phagocytic NADPH oxidase by inducing the expression of gp91phox. J Biol Chem. 2006;281(9):5657–67. https://doi.org/10.1074/jbc.M506172200.
60. Manea A, Manea SA, Gafencu AV, Raicu M. Regulation of NADPH oxidase subunit p22(phox) by NF-kB in human aortic smooth muscle cells. Arch Physiol Biochem. 2007;113(4–5):163–72. https://doi.org/10.1080/13813450701531235.
61. Manea A, Tanase LI, Raicu M, Simionescu M. Jak/STAT signaling pathway regulates nox1 and nox4-based NADPH oxidase in human aortic smooth muscle cells. Arterioscler Thromb Vasc Biol. 2010;30(1):105–12. https://doi.org/10.1161/ATVBAHA.109.193896.
62. Manea SA, Vlad ML, Rebleanu D, Lazar AG, Fenyo IM, Calin M, Simionescu M, Manea A. Detection of vascular reactive oxygen species in experimental atherosclerosis by high-resolution near-infrared fluorescence imaging using VCAM-1-targeted liposomes entrapping a fluorogenic redox-sensitive probe. Oxid Med Cell Longev. 2021;2021:6685612. https://doi.org/10.1155/2021/6685612
63. Brandes RP, Rezende F, Schröder K. Redox regulation beyond ROS: why ROS should not be measured as often. Circ Res. 2018;123(3):326–8. https://doi.org/10.1161/CIRCRESAHA.118.313146.
64. Christ A, Günther P, Lauterbach MAR, Duewell P, Biswas D, Pelka K, Scholz CJ, Oosting M, Haendler K, Baßler K, Klee K, Schulte-Schrepping J, Ulas T, Moorlag SJCFM, Kumar V, Park MH, Joosten LAB, Groh LA, Riksen NP, Espevik T, Schlitzer A, Li Y, Fitzgerald ML, Netea MG, Schultze JL, Latz E. Western diet triggers NLRP3-dependent innate immune reprogramming. Cell. 2018;172(1–2):162–e17514. https://doi.org/10.1016/j.cell.2017.12.013.
65. Chinetti-Gbaguidi G, Colin S, Staels B. Macrophage subsets in atherosclerosis. Nat Rev Cardiol. 2015;12(1):10–7. https://doi.org/10.1038/nrcardio.2014.173.
66. Cathcart MK. Regulation of superoxide anion production by NADPH oxidase in monocytes/macrophages: contributions to atherosclerosis. Arterioscler Thromb Vasc Biol. 2004;24(1):23–8. https://doi.org/10.1161/01.ATV.0000097769.47306.12.
67. Yuan R, Zhang W, Nie P, Lan K, Yang X, Yin A, Xiao Q, Shen Y, Xu K, Wang X, Pan X, Shen L, He B. Nur77 deficiency exacerbates macrophage NLRP3 inflammasome-mediated inflammation and accelerates atherosclerosis. Oxid Med Cell Longev. 2022;2022:2017815. https://doi.org/10.1155/2022/2017815.

Publisher's note